AD-A097 773 DAVID W TAYLOR NAVAL SHIP RESEARCH AND DEVELOPMENT CE--ETC F/G 20/4
EFFECTIVE WAKE: THEORY AND EXPERIMENT.(U)
APR 81 T T HUANG, N C GROVES

UNCLASSIFIED DTNSRDC-81/033 NL

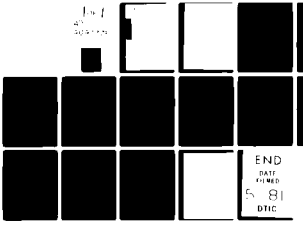

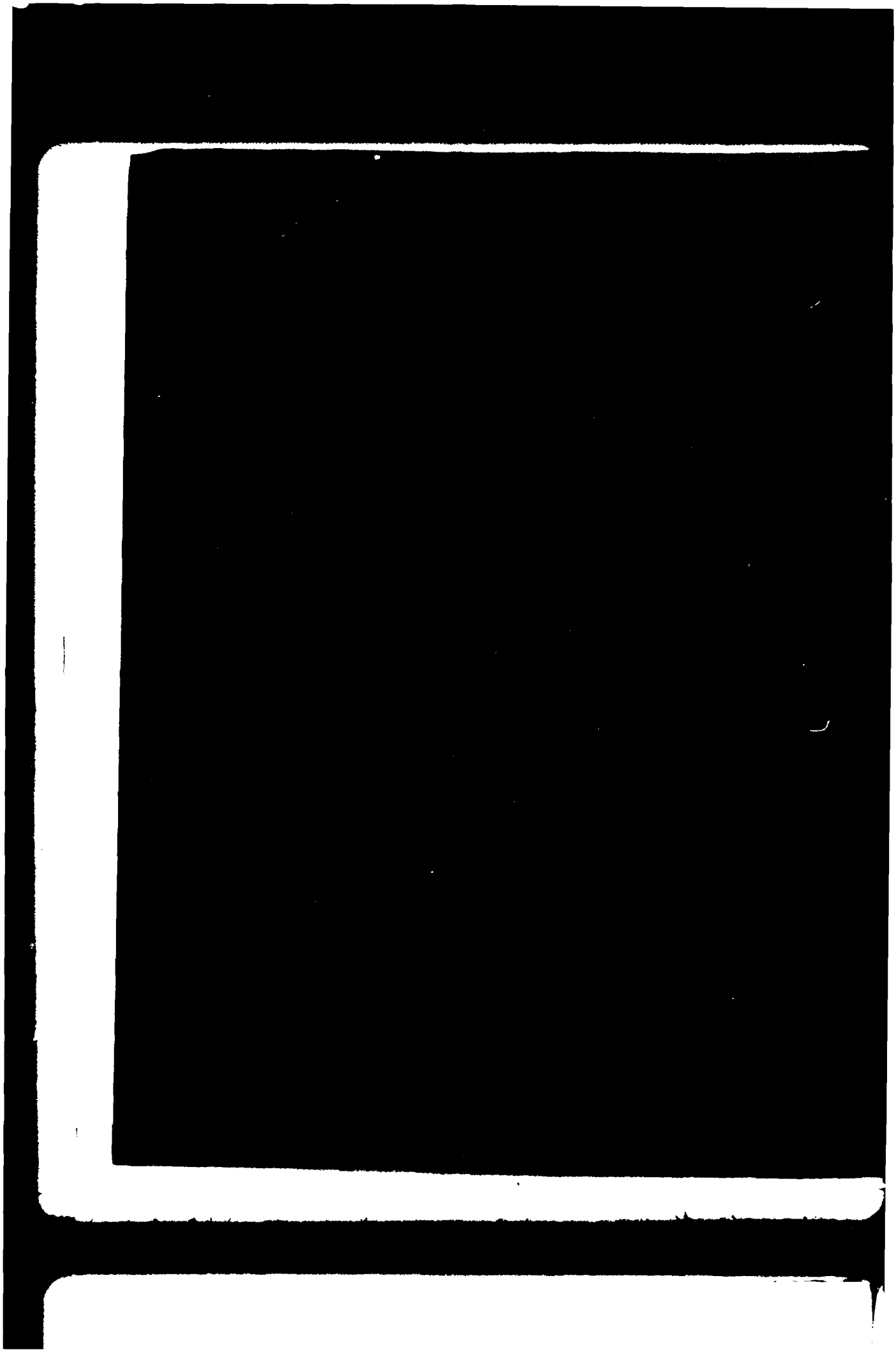

UNCLASSIFIED

SECURITY CLASSIFICATION OF THIS PAGE (When Data Entered)

REPORT DOCUMENTATION PAGE		READ INSTRUCTIONS BEFORE COMPLETING FORM
1. REPORT NUMBER DTNSRDC-81/033	2. GOVT ACCESSION NO.	3. RECIPIENT'S CATALOG NUMBER
4. TITLE (and Subtitle) EFFECTIVE WAKE: THEORY AND EXPERIMENT		5. TYPE OF REPORT & PERIOD COVERED Formal 6. PERFORMING ORG. REPORT NUMBER
7. AUTHOR(s) Thomas T. Huang and Nancy C. Groves		8. CONTRACT OR GRANT NUMBER(s)
9. PERFORMING ORGANIZATION NAME AND ADDRESS David W. Taylor Naval Ship Research and Development Center Bethesda, Maryland 20084		10. PROGRAM ELEMENT, PROJECT, TASK AREA & WORK UNIT NUMBERS Program Element 61152N Task Area ZR0230101 Work Unit 1552-103
11. CONTROLLING OFFICE NAME AND ADDRESS		12. REPORT DATE April 1981 13. NUMBER OF PAGES 23
14. MONITORING AGENCY NAME & ADDRESS(if different from Controlling Office)		15. SECURITY CLASS. (of this report) UNCLASSIFIED 15a. DECLASSIFICATION/DOWNGRADING SCHEDULE

16. DISTRIBUTION STATEMENT (of this Report)

APPROVED FOR PUBLIC RELEASE: DISTRIBUTION UNLIMITED

17. DISTRIBUTION STATEMENT (of the abstract entered in Block 20, if different from Report)

18. SUPPLEMENTARY NOTES

19. KEY WORDS (Continue on reverse side if necessary and identify by block number)

Propulsor/Hull Interaction
Axisymmetric Bodies
Turbulent Boundary Layers
Thick Stern Boundary Layer
Effective Wake

20. ABSTRACT (Continue on reverse side if necessary and identify by block number)

An improved theoretical method is presented for computing the effective wake of propulsors operating in thick stern boundary layers on axisymmetric bodies. The hydrodynamic interaction between the nominal velocities upstream of the propulsor and at the propulsor location is assumed to be inviscid in nature and the total energy is assumed to be

(Continued on reverse side)

DD FORM 1 JAN 73 1473 EDITION OF 1 NOV 65 IS OBSOLETE
S/N 0102-LF-014-6601

UNCLASSIFIED

SECURITY CLASSIFICATION OF THIS PAGE (When Data Entered)

(Block 20 continued)

conserved along a given streamline with and without the propulsor in operation. Theoretical predictions using the method are compared with experimental data obtained in the United States and Japan for five different propulsor/axisymmetric body configurations. For all five cases examined, the computed total velocity profiles immediately upstream of the propulsor (with the propulsor in operation) are in good agreement with the measured values. In addition, the volume-mean values of effective velocity profiles computed from the measured nominal velocity profiles are in good agreement with the measured values of the Taylor wake fraction ($1-w_T$) for all five nominal wake distributions over a wide range of propulsor thrust loading coefficients.

TABLE OF CONTENTS

LIST OF FIGURES

LIST OF TABLES

Effective Wake : Theory and Experiment

Thomas T. Huang and Nancy C. Groves
David W. Taylor Naval Ship Research and Development Center
Bethesda, Maryland, U.S.A.

ABSTRACT

An improved theoretical method is presented for computing the effective wake of propulsors operating in thick stern boundary layers on axisymmetric bodies. The hydrodynamic interaction between the nominal velocities upstream of the propulsor and at the propulsor location is assumed to be inviscid in nature and the total energy is assumed to be conserved along a given streamline with and without the propulsor in operation. Theoretical predictions using the method are compared with experimental data obtained in the United States and Japan for five different propulsor/axisymmetric body configurations. For all five cases examined, the computed total velocity profiles immediately upstream of the propulsor (with the propulsor in operation) are in good agreement with the measured values. In addition, the volume-mean values of effective velocity profiles computed from the measured nominal velocity profiles are in good agreement with the measured values of the Taylor wake fraction ($1-w_T$) for all five nominal wake distributions over a wide range of propulsor thrust loading coefficients.

1. INTRODUCTION

The velocity profile at the location of the propulsion device in the absence of a propulsor is called the nominal velocity profile. The effective inflow velocity distribution experienced by the propulsor depends on the mutual interaction of the propulsor (loading distribution and geometric characteristics) and the stern boundary layer. It can be significantly different from the nominal velocity distribution. In the design of a wake-adapted propulsor, the radial distribution of effective inflow velocity is often estimated by ratioing the measured nominal circumferential-mean axial profile up or down by a constant factor. The factor is sometimes taken to be $(1-w_T)/(1-w_N)$, where w_T is the Taylor wake fraction and w_N is the measured volume-mean nominal wake. Naval architects derive the Taylor wake fraction from propeller open water curves on the basis of thrust identity between propeller powering experiments in open water and behind the ship model.

The constant-factor empirical approach for obtaining effective inflow distribution is not based on a rational hydrodynamic theory. Until recently, detailed velocity surveys in the presence of an operating propulsor were not available, and the actual distribution of effective velocity into a propulsor had not been examined fully. Providing the correct distribution of effective inflow for wake-adapted propulsor design is essential to meeting the ever increasing demand for improving propulsion performance and energy conservation. In order for a propulsor to produce a required thrust to power a ship with minimum power and minimum cavitation at a prescribed propulsor rotational speed, the effective velocity distribution used in the propulsor design must be very accurate.

In 1976, a Laser Doppler Velocimeter (LDV) was successfully used by Huang et al.[1] to measure velocity profiles very close to the propulsor. The measured velocity profiles, stern pressure distributions, and stern shear stress distributions with and without an operating propulsor provided the necessary clues to the proper understanding of the interaction between a propulsor and stern boundary layer on axisymmetric bodies. The influence of propulsors on axisymmetric stern boundary layers was found to be contained within a limited region extending two propulsor diameters upstream of the propulsor. The propulsor/stern boundary layer interaction was found to be inviscid in nature. The inviscid approximation computer program developed by Huang et al.[1] predicted very well the measured total velocities in front of the operating propulsor. Subsequent detailed measurements of the velocity profiles with and without a propulsor operating in two axisymmetric wakes were made by Nagamatsu and Tokunaga.[2] An inviscid approximation again predicted well the measured total velocities in front of the operating propulsor.

Schetz and Favin[3,4] have formulated a numerical procedure based on the full Navier-Stokes equations to compute the flow near body/propulsor configurations. The computed axial velocities at two propulsor diameters downstream of the propulsor compared satisfactorily with the measured results. This numerical procedure has not been applied to the computation of effective wake in design of wake-adapted propulsors.

The influence of a stern-mounted propulsor on the flow field past bodies of revolution and a flat plate was measured by Hucho,[5,6,7] although no attempt was made to ac-

tually calculate the effective wake distribution. Other investigations related to this subject were made by Wertbrecht,[8] Hickling,[9] Tsakonas and Jacobs,[10] and Wald.[11] Methods to estimate effective wake were proposed by Raestad,[12] Nagamatsu and Sasajima,[13] and Titoff and Otlesnov.[14] The only known previous effort to theoretically address this problem is due to D.M. Nelson* who developed a computer program for calculating the effective wake from the measured nominal wake and static pressure distribution across the boundary layer.

In the present paper, an improved method for computing effective wake distribution from the measured nominal wake distribution is derived. Serious effort has been made in this work to compare the theoretical velocity predictions with velocity distributions measured by an LDV or a five-hole pitot probe immediately upstream of an operating propulsor. For all five cases examined, the computed total velocities upstream of the operating propulsors are in good agreement with the measured values.

The computed volume-mean effective wake distributions are shown to compare favorably with the measured Taylor wake fractions derived from self-propulsion experiments of five different nominal wakes. A considerable amount of experimental data and relevant computational results are tabulated to permit the independent assessment of the present method by other investigators.

2. THEORY

2.1 Propulsor/Stern Boundary Layer Interaction

The experimental data given in References 1 and 2 allow one to conclude that the influence of propulsors on upstream stern boundary layers is detectable only within two propulsor diameters upstream of the propulsor. Upstream of the propulsor, the mean circumferential velocity, v_θ, is identically equal to zero on an axisymmetric body both with and without the propulsor in operation. The following assumptions are made to derive a theoretical approximation of the hydrodynamic interaction between a propulsor and a thick stern boundary layer upstream of the propulsor: (a) the flow is axisymmetric and the fluid is incompressible; (b) the interaction of propulsor and nominal velocity profile is considered to be inviscid in nature; thus, propulsor-induced viscous losses and turbulent Reynolds stresses are neglected; (c) the conventional boundary-layer assumption, $\partial v_r/\partial x \ll \partial u_x/\partial r$ is assumed to be valid for the nominal boundary layer in the absence of a propulsor; and (d) upstream of the propulsor, no energy is added to the fluid by the propulsor, and the propulsor-induced velocity field upstream of the propulsor is irrotational. The theoretical formulation of propulsor/stern boundary layer interaction subject to the above assumptions has already been given by Huang et al.,[1] and will only be briefly outlined here.

The vector equation of steady motion for an inviscid fluid is given by (see, for example, Reference 15)

$$\vec{V} \times \vec{\omega} = \frac{1}{\varrho} \text{grad } H, \qquad (1)$$

where $\vec{V}$ is the fluid velocity, $\vec{\omega} = \nabla \times \vec{V}$ is the vorticity vector, and $H = p + \frac{1}{2}\varrho(\vec{V} \cdot V)$ is the total head, with ϱ mass density and p pressure. For cylindrical polar coordinates (r, θ, x) with $\vec{V} = (v_r, v_\theta = 0, u_x)$, the radial component of Equation (1) may be written[1] as

$$u_x \left(\frac{\partial u_x}{\partial r} - \frac{\partial v_r}{\partial x} \right) = \frac{1}{\varrho} \frac{\partial H}{\partial \psi} \frac{d\psi}{dr} = \frac{r u_x}{\varrho} \frac{\partial H}{\partial \psi}, \qquad (2)$$

*Private communication, unpublished

where ψ is the stream function for an incompressible axisymmetric flow defined by

$$u_x = \frac{1}{r} \frac{\partial \psi}{\partial r},$$

$$v_r = -\frac{1}{r} \frac{\partial \psi}{\partial x}.$$

Since the flow velocities are increased due to the action of the propulsor, stream surfaces are shifted closer to the body surface. As shown in Figure 1, a typical stream surface moves inward from r to r_p while the resultant velocity is higher than the nominal velocity. The resultant velocity u_p, as would be measured in front of the propulsor, will be called the total velocity.

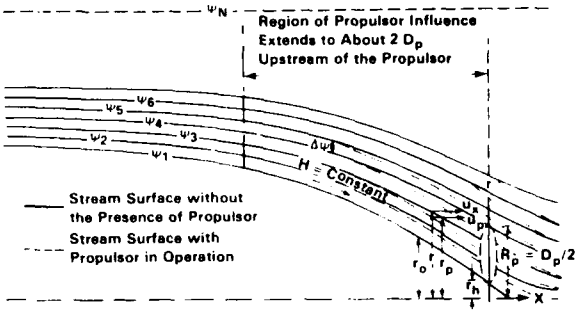

Figure 1 – Definition Sketch for Propulsor Stern Boundary Layer Interaction

Since no energy is added to the upstream fluid by the propulsor and since we assume no change of viscous losses due to propulsor induction effects, the total pressure head within a given stream annulus upstream of the propulsor remains constant with the propulsor (denoted by a subscript p) and without the propulsor in operation; thus, upstream of the propulsor

$$\frac{1}{\varrho} \frac{\partial H}{\partial \psi} = \frac{1}{\varrho} \left(\frac{\partial H}{\partial \psi} \right)_p$$

or from Equation (2)

$$\frac{\omega_\theta}{r} = \frac{1}{r} \left(\frac{\partial u_x(r)}{\partial r} - \frac{\partial v_r(r)}{\partial x} \right) =$$

$$\frac{1}{r_p} \left[\frac{\partial u_p(r_p)}{\partial r_p} - \frac{\partial (v_r(r_p) + v_{pr}(r_p))}{\partial x} \right], \qquad (3)$$

where ω_θ is the θ-component of the vorticity vector. The value of ω_θ/r must therefore be conserved along the stream annulus with and without an operating propulsor. The radial velocity with the propulsor in operation is assumed equal to $v_r + v_{pr}$, where v_r is the radial velocity without propulsor and v_{pr} is the circumferential-average propulsor-induced radial velocity. Since the propulsor-induced velocity field is assumed to be irrotational, we require

$$(\vec{\nabla} \times \vec{V}_{pi})_\theta = \frac{\partial v_{pr}}{\partial x} - \frac{\partial u_a}{\partial r_p} = 0,$$

where $\vec{V}_{pi}$ is the resultant propulsor-induced velocity, and u_a is the circumferential-average propulsor-induced axial velocity. Substitution into Equation (3) yields a simple relationship for the location of the new stream surface r_p

$$\frac{1}{r}\frac{\partial u_x}{\partial r} = \frac{1}{r_p}\left(\frac{\partial u_p}{\partial r_p} - \frac{\partial u_a}{\partial r_p}\right) - \left[\frac{1}{r_p}\frac{\partial v_r(r_p)}{\partial x} - \frac{1}{r}\frac{\partial v_r(r)}{\partial x}\right] . \quad (4)$$

The normal boundary-layer approximation $\partial v_r/\partial x \ll \partial u_x/\partial r$ is now assumed to be valid for the nominal velocity profiles. In order to check this assumption, the radial nominal velocity profiles were measured by a TSI, Inc. Model 1241 "X" - wire at two axial planes, one immediately upstream ($x/D_p = -0.227$) of the propulsor and one on the propulsor plane. The values of $\partial v_r/\partial x$ determined from velocity measurements on Afterbodies 1 and 2 of Reference 16 were found to be less than 0.05 $\partial u_x/\partial r$. The radial velocity v_r was found to vary very slowly across the boundary layer.[16] Therefore, we may assume that $v_r(r) \cong v_r(r_p)$. Furthermore, the value of $(r-r_p)/r_p$ represents the percentage change in radial location of a given streamline with and without the propulsor operating; its value is found to be less than 0.2 for most of the cases considered. Thus, the order of magnitude of the last term in Equation (4) can be estimated as

$$\frac{\frac{1}{r_p}\frac{\partial v_r(r_p)}{\partial x} - \frac{1}{r}\frac{\partial v_r(r)}{\partial x}}{\frac{1}{r}\frac{\partial u_x}{\partial r}} \cong \frac{\frac{\partial v_r(r)}{\partial x}\frac{r-r_p}{rr_p}}{\frac{1}{r}\frac{\partial u_x}{\partial r}} < 0.01$$

and, therefore, will be neglected in the following analysis. Equation (4) then reduces to

$$\frac{1}{r}\frac{\partial u_x}{\partial r} = \frac{1}{r_p}\left(\frac{\partial u_p}{\partial r_p} - \frac{\partial u_a}{\partial r_p}\right) . \quad (5)$$

Within a given stream annulus the massflow is constant with or without a propulsor operating. Thus, at a given axial location x, we may write,

$$d\psi = ru_x dr = r_p u_p dr_p . \quad (6)$$

Inserting this expression into Equation (5) yields

$$u_x du_x = u_p d(u_p - u_a) . \quad (7)$$

Equations (6) and (7) are the governing equations for the propulsor and stern boundary-layer interaction. The nominal velocity, $u_x(r)$, and the circumferential-average propulsor-induced axial velocity, $u_a(r_p)$, can be used to obtain the new location of the stream surface r_p with total velocity u_p. In Equation (6), the values of r and r_p are equal on the body surface. Far outside of the boundary layer, the flow is uniform without any vorticity. Then we have $du_x = 0$ as $r \to \infty$ in Equation (6), which implies $d(u_p - u_a) = 0$, and $u_p - u_a$ = constant = V (ship speed), or $u_p = V + u_a$, since u_a is zero and u_p has to be equal to V as $r \to \infty$.

Similarily, for an open propulsor in uniform flow, $du_x = 0$ in equation (7), and we have $u_p = V + u_a$. The total velocity u_p for an open propulsor in uniform flow is the sum of the uniform ship speed V and the propulsor-induced velocity u_a without any interaction.

If the nominal velocity field is irrotational, the left-hand side of Equation (3) must be zero; thus, the right-hand side of Equation (3) becomes

$$\frac{\partial u_p(r_p)}{\partial r_p} - \frac{\partial v_r(r_p)}{\partial x} - \frac{\partial v_{pr}(r_p)}{\partial x} = 0 .$$

Using the irrotationality condition applies to the nominal velocity as well as propulsor-induced velocity fields, e.g.

$$\frac{\partial v_{pr}(r_p)}{\partial x} = \frac{\partial u_a(r_p)}{\partial r_p} \text{ and } \frac{\partial v_r(r_p)}{\partial x} = \frac{\partial u_x(r_p)}{\partial r_p} .$$

The above equation becomes

$$\frac{\partial}{\partial r_p}\left[u_p(r_p) - u_x(r_p) - u_a(r_p)\right] = 0 ,$$

or

$$u_p(r_p) = u_x(r_p) + u_a(r_p) .$$

Thus, the total velocity u_p for a propulsor operating in an irrotational nominal velocity field is the sum of the corresponding nominal velocity and the propulsor-induced velocity without any additional interaction.

2.2 Effective Velocities

In current propulsor design and performance prediction practice, only the measured model nominal velocity profile is available. The full-scale nominal velocity profile can then be estimated as the sum the measured model nominal velocity profile plus an appropriate Reynolds-number correction. The nominal velocity profile for either the model or the full-scale propulsor is assumed to be available at the outset. The present theory can be applied to obtain the effective velocity distribution using the nominal velocity profile as input.

If the effective velocity is defined to be the total velocity with the propulsor in operation minus the propulsor-induced axial velocity, $u_e = u_p - u_a$, then Equation (7) becomes

$$u_x du_x = (u_e + u_a)du_e . \quad (8)$$

At large radial distances from the propulsor axis ($r \to \infty$), the value of the propulsor-induced velocity becomes zero and, hence, the effective velocity is equal to the nominal velocity as $r \to \infty$. The finite-difference form of Equation (8) can be written as

$$[u_{x_{i+1}} + u_{x_i}][u_{x_{i+1}} - u_{x_i}] = [u_{e_{i+1}} + u_{a_{i+1}} + u_{e_i} + u_{a_i}][u_{e_{i+1}} - u_{e_i}] ,$$

or

$$u_{e_i} = \sqrt{u_{e_{i+1}} + \left(\frac{u_{a_{i+1}} + u_{a_i}}{2}\right)^2 + (u_{x_i}^2 - u_{x_{i+1}}^2)} - \frac{u_{a_{i+1}} + u_{a_i}}{2} . \quad (9)$$

In practice, the nominal velocities are known from the innermost radius of the propulsor to a radial position (e.g., $r \geq 3.0$ R_p) large enough for the propulsor-induced axial velocity u_a to be zero. The value of the effective velocity at that point is equal to the nominal velocity. This condition can be used to solve the effective velocity in Equation (9) step by step from this initial radial position inward towards the body surface. The nominal velocity at the hub of the propulsor is usually taken to be the linearly extrapolated value of the measured nominal velocities near the body surface rather than zero in order to avoid an unnecessarily large number of computational grid points near the body surface.

Since the induced velocity u_a is not known initially, the present theory can be applied in an iterative procedure to propulsor design of performance prediction. The circumferential-average propulsor-induced axial velocity u_a will be assumed to

be the same within the same stream annulus with and without the propulsor in operation in every iteration.

In conventional propulsor design, when the nominal wake distribution is given and either the propulsor thrust at a given speed or the delivered shaft power is given, the following procedure may be followed:

(a) First, estimate the thrust loading coefficient C_{TS} of the propulsor and then estimate the propulsor-induced axial velocity by using the actuator disk approximation,[17] i.e.,

$\frac{r}{R_p}$	0.2	0.3	0.4	0.5	0.6	0.7	0.8	0.9	1.0
$\frac{u_a}{VC_{TS}}$	0.147	0.206	0.254	0.290	0.311	0.315	0.293	0.233	0

An initial estimate of effective velocities can then be obtained by solving Equation (9).

(b) The conventional propulsor lifting-line computional method[18,19,20] may be used to design a propulsor to operate in the estimated effective velocity profile u_e with a prescribed nondimensional circulation distribution G which produces the required thrust. An improved solution estimate of the circumferential-average propulsor-induced axial velocity, u_a, can be computed from the output of the lifting line computer program[19] by a simple integration,[21]

$$\frac{u_a}{V} = -\frac{K}{2}\int_{\tilde{r}_h}^{1}\frac{d\tilde{G}(\tilde{r})}{d\tilde{r}}\frac{d\tilde{r}}{\tilde{r}\tan\beta_i(\tilde{r})}, \qquad (10)$$

where $G = \Gamma/2\pi R_p V$, $\tan\beta_i = (u_a + \tilde{u}_a)/(\Omega\tilde{r}R_p - \tilde{u}_\phi)$, K is the number of blades, Ω is the propulsor angular velocity, $\tilde{r} = r/R_p$, $\tilde{r}_h$ is the dimensionless hub radius, and $\tilde{u}_a$ and $\tilde{u}_\phi$ are the axial and tangential propulsor induced velocities at lifting line, respectively.

(c) A new effective velocity profile can be obtained by using the new lifting-line solution of u_a in Equation (9).

(d) Steps (b) and (c) are repeated until the values of G and u_a converge to within some specified tolerance. Two iterations have been found to be sufficient for preliminary design.

(e) If a final lifting surface design[20,22,23] is required, the final solution of circumferential-average propulsor-induced axial velocity, u_a, at the propeller plane can be calculated by using a field-point velocity program[20] which includes lifting surface corrections and thickness distributions. The final effective velocity profile is obtained by using the final lifting-surface solution of u_a in Equation (9).

For calculation of the performance of a propulsor of given geometry and rpm, a computational method[24] is available to predict G and $\tan\beta_i$ for estimated values of u_e. A new effective velocity profile can be calculated using the new induced velocity u_a computed from the field-point velocity program.[20]

2.3 Total Velocities Upstream of Propulsor

The total velocities at the propulsor plane are rather difficult to measure. Therefore, in order to evaluate the present theory a comparison of total velocity u_p between theory and experiment must be made immediately upstream of the propulsor. The total velocity is $u_p = u_a + u_e$ where u_e is solved by Equation (9) and the value of the propulsor-induced velocity u_a must be calculated at the position where the total velocities are measured. The new radial position for u_p can be obtained from Equation (6). The nominal velocity u_x can be approximated very accurately over a small increment of radius dr as a linear function of r. Although the velocity at the wall is zero, the velocity profile in the present approximation will be extrapolated linearly toward the wall, resulting in a nonzero velocity at the wall. Since u_x and u_p can be approximated locally by a linear function of r and r_p, the mass flux within the stream tube annulus given by $dr = r_{i+1} - r_i$ and $dr_p = r_{p_{i+1}} - r_{p_i}$ can be integrated from Equation (6) as

$$\psi_{i+1} - \psi_i = \Delta\psi_i = \int_{r_i}^{r_{i+1}} ru_x dr = \int_{r_{p_i}}^{r_{p_{i+1}}} r_p u_p dr_p$$

with $u(r) = u_i + [(r - r_i)/(r_{i+1} - r_i)](u_{i+1} - u_i)$ and $r_i \le r \le r_{i+1}$

to obtain the finite difference form of Equation (6) as

$$(r_{i+1}^2 - r_i^2)\left[(2u_{x_{i+1}} + u_{x_i}) - (u_{x_{i+1}} - u_{x_i})\frac{r_i}{r_{i+1} + r_i}\right] = (r_{p_{i+1}}^2 - r_{p_i}^2)\left[(2u_{p_{i+1}} + u_{p_i}) - (u_{p_{i+1}} - u_{p_i})\frac{r_{p_i}}{r_{p_{i+1}} + r_{p_i}}\right] \qquad (11)$$

At the body surface $r_1 = r_{p_1}$. This condition can be used to solve for $r_{p_{i+1}}$ step by step from the body surface outward, e.g.

$$r_{p_{i+1}} = \frac{C + \sqrt{C^2 - 4BD}}{2B} \qquad (12)$$

where $B = 2u_{p_{i+1}} + u_{p_i}$

$C = -r_{p_i}(u_{p_{i+1}} - u_{p_i})$

$D = -r_{p_i}^2(u_{p_{i+1}} - 2u_{p_i}) - F$

$F = (r_{i+1}^2 - r_i^2)(2u_{x_{i+1}} + u_{x_i}) - r_i(u_{x_{i+1}} - u_{x_i})(r_{i+1} - r_i)$

Both the effective velocity u_{e_i} and the new radial position $r_{p_{i+1}}$ for the total velocity $u_{p_{i+1}} = u_{x_{i+1}} + u_{a_{i+1}}$ are the simple solutions of the quadratic Equations (9 and 12). The effective velocity is solved (independent of r_p) inward from a large radial position where the propulsor-induced velocity is zero. Once the values of u_e are obtained, the new radial position $r_{p_{i+1}}$ can be solved from the body surface outward. These two solutions are decoupled without any need for employing an iterative numerical procedure. These solutions can readily be incorporated in most propulsor design practices.

3. EXPERIMENT

3.1 Two Propulsors in Five Nominal Wakes

The experimental data used to evaluate the present theory are derived from two propulsors operating in five different nominal wakes. The geometrical characteristics of the propulsor used at DTNSRDC, denoted Propulsor T, are given in Reference 1 and those of the propulsor used at Nagasaki Experimental Tank by Nagamatsu and Tokunaga, denoted Propulsor J, are given in Reference 2.

Three axisymmetric bodies, designated as Models 1, C, and D, were used to generate thick stern boundary layers for Propulsor T. The offsets of the three models are given in Tables 1 through 3. The propulsor was located at x/L = 0.983, where x is the axial distance from the nose and L is the total body length. The ratio of the propulsor radius to the maximum hull radius, R_p/r_{max}, is 0.545 for Model 1 and 0.484 for Models C and D. The maximum radius of the model (r_{max}) is 13.97 cm for Model 1 and 31.18 cm for Models C and D. The three models were constructed of molded fiberglass; specified profile tolerances were held to less than ± 0.4 mm, all

imperfections were removed, meridians were faired, and the fiberglass was polished to a 0.64 micron rms surface finish.

One axisymmetric body was constructed by Nagamatsu and T. Kunaga[2] for their investigation. The total length of the body was 3.085 m and the maximum radius was 10.66 cm. The propulsor was located at 2.57 propeller diameters downstream of the after perpendicular. A wire mesh was wrapped around the aft portion of the parallel middle body. The nominal wakes without and with the wire mesh will be designated as wakes A and B, respectively. The value of R_p/r_{max} was 0.610.

The measured distributions of the nominal axial velocities at the propulsor plane for the five wakes are shown in Figure 2. There is considerable variation in the nominal velocity distributions among the five wakes selected for the present investigation.

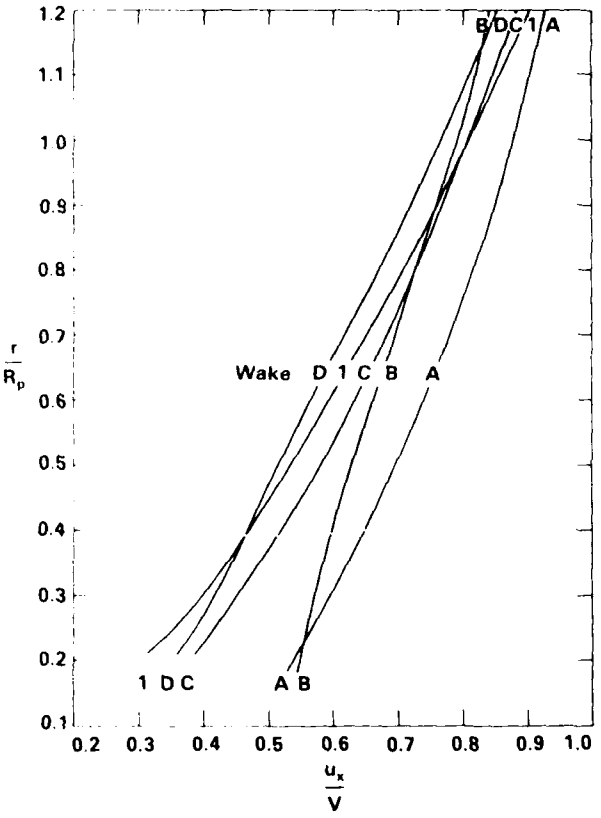

Figure 2 – Measured Nominal Axial Velocity Profiles of the Five Nominal Wakes

3.2 Experimental Technique

The experimental investigation of Models 1, C, and D was conducted in the DTNSRDC anechoic wind tunnel. The wind tunnel has a 2.438- by 2.438-m test section with a maximum air speed of 61 m/s. The model was supported by two streamlined struts separated by roughly one-third of the model length. The upstream strut had a 15-cm chord and the downstream strut had a 3-cm chord. The distrubances generated by the supporting struts were within the region below the horizontal centerplane. All the measurements of the nominal and the total velocities were made in the vertical centerplane along the upper meridian and there was little extraneous effect from the supporting struts. Each stern of the model protruded from the closed-jet working section of the wind tunnel into the anechoic chamber (6.4 x 6.4 x 6.4 m) located upstream of the diffuser. Propulsor T was driven by a 9-kW high-speed motor mounted inside the stern of the model. The rotational speed of the propulsor shaft was measured by a magnetic pick-up.

Time-average nominal velocities at the propulsor plane and at a plane immediately upstream of the propulsor plane in the absence of the propulsor were measured by a Laser Doppler Velocimeter (LDV) and checked by a TSI, Inc. Model 1241 "X" wire monitored by a two-channel TSI Model 1050-1 hot-wire anemometer.[16] The axial velocity profiles inside the stern boundary layer measured by the LDV and by the hot-wire anemometer were found to agree within two percent of the free-stream velocity. The total velocities immediately upstream of the propulsor were measured by the LDV with the propulsor in operation. Some of the data have already been reported in Reference 1. Most data presented in this investigation were measured after the publication of Reference 1 although the same LDV measurement techniques were used. The overall accuracy of the measured axial velocities by the LDV is about two percent of the free-stream velocity.

In the investigation of Nagamatsu and Tokunaga,[2] the model was also supported by two struts and propulsor J was mounted on and driven by the dynamometer used for open-water propulsion testing. The experiments were conducted in a towing tank. The propulsor plane was located at 5.13 R_t downstream of the after perpendicular of the model; the model centerline depth of submergence was 4.6 R_t, where R_t is the radius of the propulsor. A five-hole pitot probe of NPL type was used to measure the axial and the radial velocities with and without the propulsor in operation. The overall accuracy of this type of pitot probe for measuring velocity is about three percent of the free-stream velocity. Standard self-propulsion and open-water experiments were conducted to determine the Taylor wake fraction.

Standard self-propulsion experiments were also conducted in the DTNSRDC model basin using a large model; the centerline depth of submergence was 1.7 R_t to avoid the effect of the free surface. The towing strut had a 20-cm chord and was located at 40-percent of body length downstream from the nose. The conditions of the self-propulsion experiments for the two propulsors operating in the five nominal wakes are tabulated in Table 4, to be discussed below.

4. RESULTS AND DISCUSSIONS

4.1 Effective Wake

The two propulsors used in the self-propulsion experiments (Table 4) were stock propulsors and were not operated at their design conditions. A propulsor performance prediction computer program[24] was used to compute the values of non-dimensional circulation G and hydrodynamic pitch angle $\tan\beta_i$ for the estimated values of u_a. The final values of $\tan\beta_i$ were scaled up or down by the ratio of the measured value of K_T to the computed value of K_T. The values of G and modified $\tan\beta_i$ were then used to compute the propulsor-induced velocities by a field-point velocity computer program[20] with a lifting-surface option. The new values of u_a were then used to compute a second estimate of the effective velocity u_e by using Equation (9). Three iterations were sufficient for the computed values of u_e to converge to within 0.2 percent accuracy. Table 4 shows the computed values of K_Q, η_D, the volume-mean effective and nominal velocities, $(u_x)_\forall$ and $(u_x)_\forall$, and the effective velocity at the 0.7 propulsor radius. The notation used in Table 4 is as follows:

$$G = \frac{\Gamma}{2\pi R_t V} = \text{non-dimensional circulation}$$

$C_{TS} = \dfrac{T}{\frac{\varrho}{2}V^2\pi R_p^2}$ = thrust loading coefficient based on ship speed

$K_T = \dfrac{T}{\varrho n^2 D^4}$ = thrust coefficient

$K_Q = \dfrac{Q}{\varrho n^2 D^5}$ = torque coefficient

$\eta_D = (1-t)\dfrac{J_v K_T}{2\pi K_Q}$ = propulsive efficiency

$J_v = \dfrac{V}{nD}$ = ship-speed advance coefficient

V = ship speed

F = circulation

T = Thrust

Q = Torque

t = Thrust deduction fraction

ϱ = mass density of the fluid

n = Rate of revolution

$D = 2R_p$ = Propulsor diameter

$[u_e]_\nabla/V = \dfrac{\int_{r_h}^{R_p} 2\pi r \frac{u_e}{V}\,dr}{\pi(R_p^2 - r_h^2)}$ = Volume-mean effective velocity ratio

$[u_x]_\nabla/V = \dfrac{\int_{r_h}^{R_p} 2\pi r \frac{u_x}{V}\,dr}{\pi(R_p^2 - r_h^2)}$ = Volume-mean nominal velocity ratio

and r_h = Hub radius of the propulsor

The experimentally determined value of the Taylor wake fraction w_T is also shown in Table 4. It is important to note that the measured values $(1-w_T)$ agree to within ± 0.03 with the computed values of the volume-mean effective velocity ratio, $[u_e]_\nabla/V$, and effective velocity ratio at 0.7 propulsor radius, $[u_e]_{r/R_p=.7}/V$, for all twelve propulsion conditions. The overall accuracy of the propulsion experiments is about ± 2%. There is no reason that the value of $(1-w_T)$ should be exactly equal to $[u_e]_\nabla/V$. However, the general agreement between the measured values of $(1-w_T)$ and the computed values of $[u_e]_\nabla/V$ for a wide variety of nominal wakes and propulsion loading conditions does provide an indirect confirmation of the *present theory*.

Typical values of the computed effective and total velocities at the plane of the propulsor are shown in Figure 3 and listed in Table 5. The final computed values of G, $\tan\beta_i$, and u_a are listed in Table 6 for the conditions used in this investigation. This information is sufficient for other investigators to perform independent calculations.

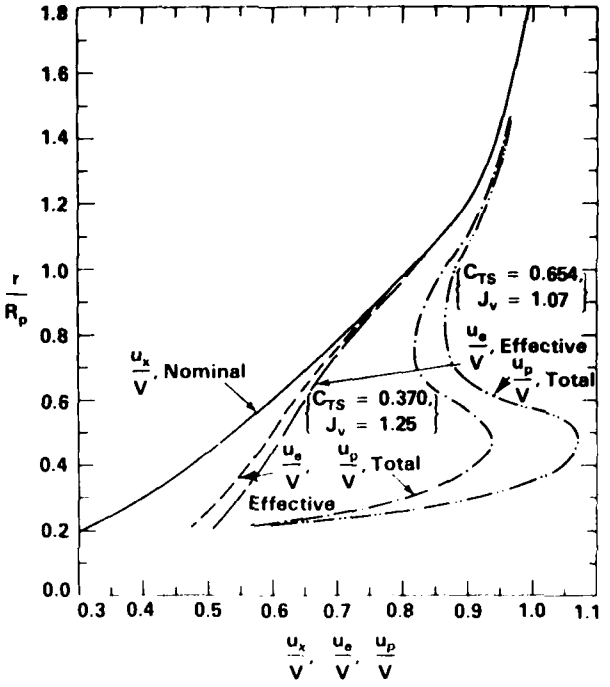

Figure 3 – Typical Total and Effective Axial Velocity Profiles Computed from the Measured Nominal Axial Velocity Profiles at the Location of Propulsor T in Wake 1

4.2 Total Velocities Upstream of Propulsor

With the final computed values of G, $\tan\beta_i$ and u_a, the field-point velocity computer program[20] with the lifting-surface option was used to compute the induced velocity u_a upstream of the propulsor. The total velocity u_p and the radial position r_p were then computed using Equations (9) and (11). The detailed results of the computation and the measured data are tabulated in Table 7. The comparisons between the measured total velocity profiles and the computed total velocity profiles are shown in Figures 4 through 9. The agreement between the measured and computed values of u_p is excellent for all cases. Thus, it may be concluded that the present inviscid approximation provides a good representation of *the complex hydrodynamic interaction between the propulsor* and the wake and can be used with confidence to calculate the effective velocity profile for a propulsor in an axisymmetric wake. The ratio of the measured total and nominal velocities shown in Figures 4 through 9 is found to be largest near the propulsor hub and to decrease toward the propulsor tip. Hence, the computed ratio of effective and nominal velocities is largest at the propulsor hub and decreases to about 1.0 at the propulsor tip, which is quite different from methods which assume that the effective wake profile is a constant multiple of the nominal wake profile.

5. CONCLUSION

In this paper, we have summarized recent experimental and theoretical investigations of the effective wake for the axisymmetric propulsor/stern boundary layer interaction problem. A comprehensive set of experimental data in tabulated form is presented for two propulsors operating in five quite different nominal wakes. The data are compared with calculations based on an inviscid propulsor/stern boundary layer interaction theory and provide valuable insights into the

manner in which the propulsor interacts with a thick stern boundary layer.

The numerical procedures for computing the effective wake and the total velocity upstream of the propulsor have been simplified to the solution of two quadratic algebraic equations. The procedure can readily be incorporated into any propulsor design and performance prediction practice.

It is shown that for twelve self-propulsion conditions covering a wide range of propulsion thrust loading coefficients, the computed volume-mean effective wakes agree well with the measured Taylor wake fractions based on thrust identity. The present inviscid propulsor/stern boundary-layer interaction theory predicts very well the measured total velocity profile immediately upstream of the operating propulsor. The computed ratio of the effective and nominal velocities is largest near the propulsor hub and decreases to about 1.0 at the propulsor tip. This is contrary to some older methods which assume that the effective wake profile is a constant multiple of the nominal wake profile.

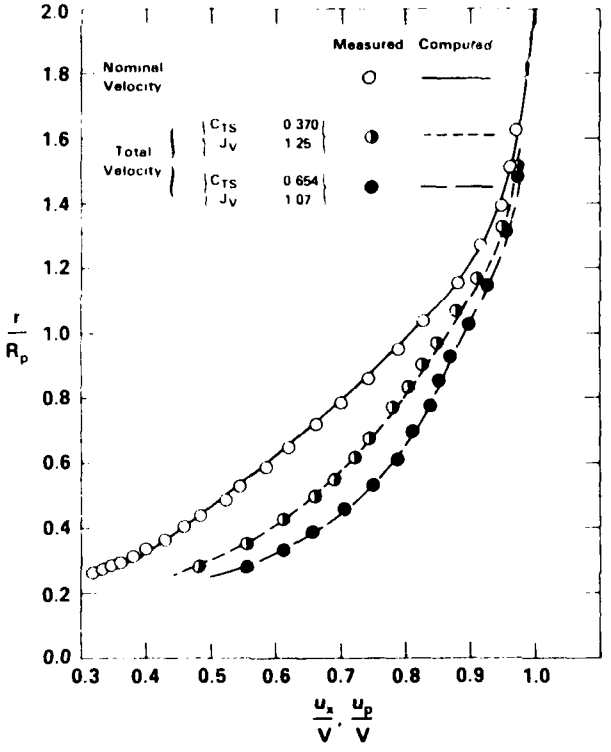

Figure 4 – Measured and Computed Axial Velocity Profiles Immediately Upstream of Propulsor (x/D_p = 0.227) With and Without Propulsor T Operated in Wake 1

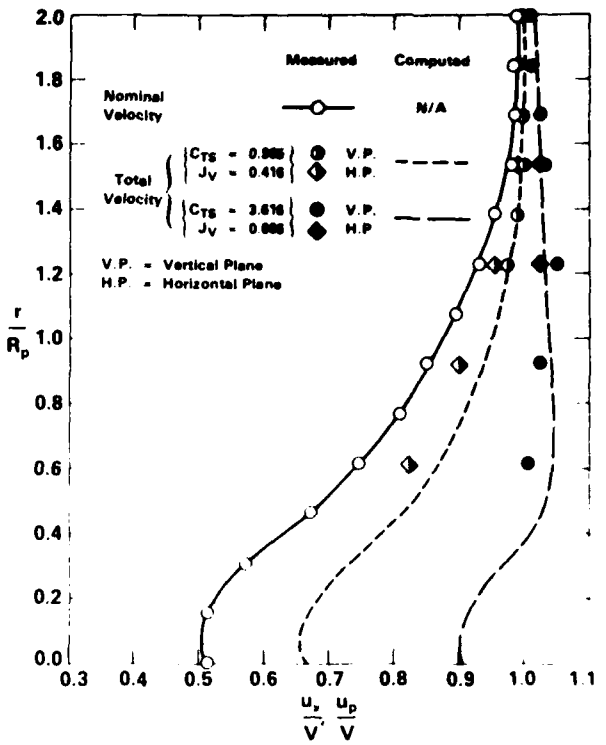

Figure 5 – Measured and Computed Axial Velocity Profiles Immediately Upstream of Propulsor (x/D_p = 0.336) With and Without Propulsor J Operated in Wake A

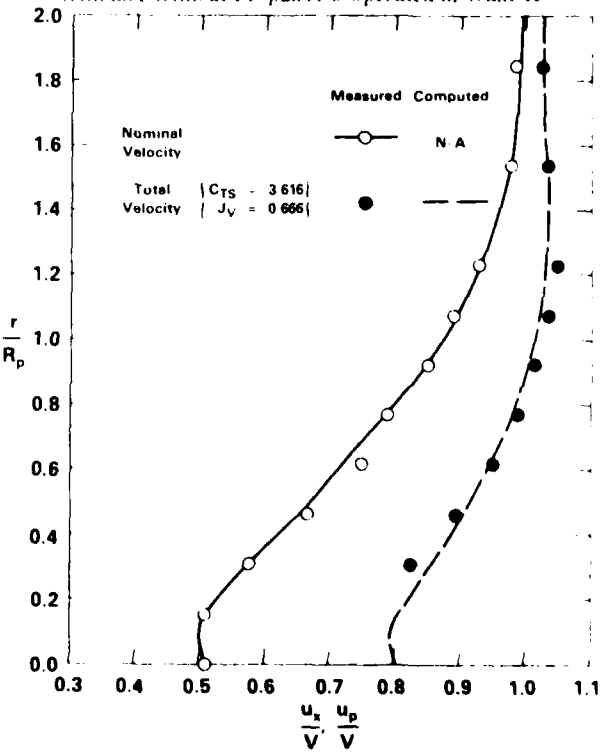

Figure 6 – Measured and Computed Axial Velocity Profiles Upstream of Propulsor (x/D_p = –0.489) With and Without Propulsor J Operated in Wake A

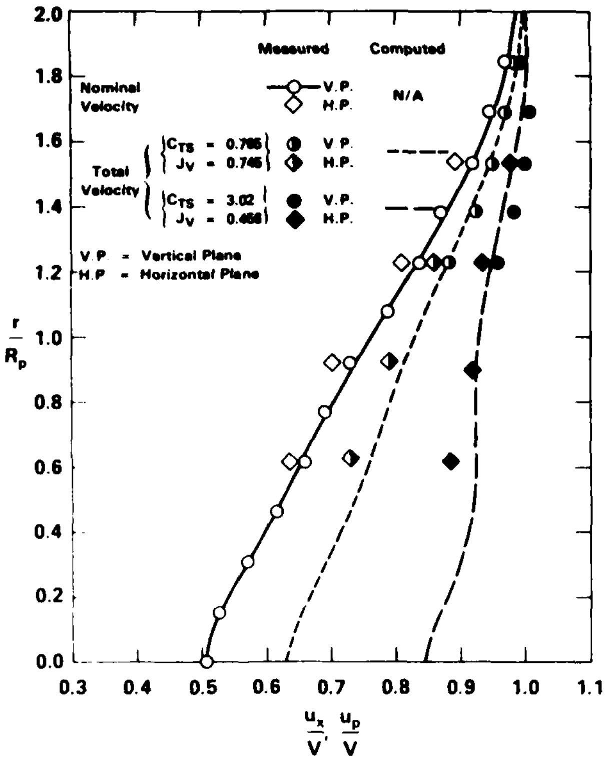

Figure 7 – Measured and Computed Axial Velocity Profiles Immediately Upstream of Propulsor (x/D_p = −0.227) With and Without Propulsor J Operated in Wake B

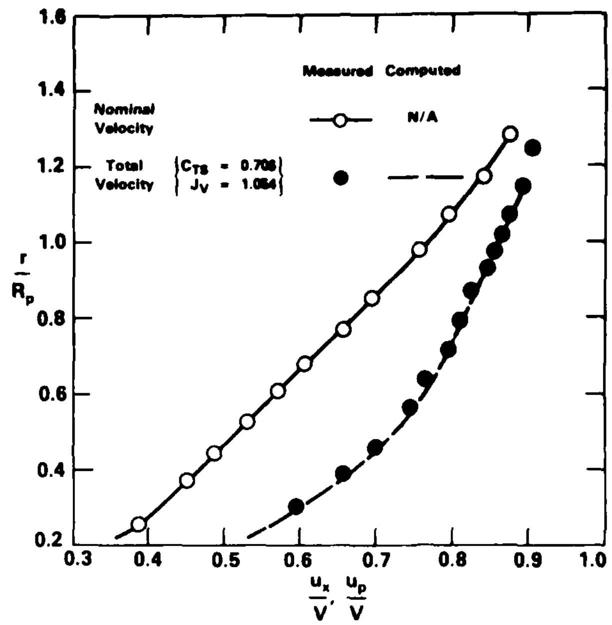

Figure 9 – Measured and Computed Axial Velocity Profiles Immediately Upstream of Propulsor (x/D_p = −0.239) With and Without Propulsor T Operated in Wake D

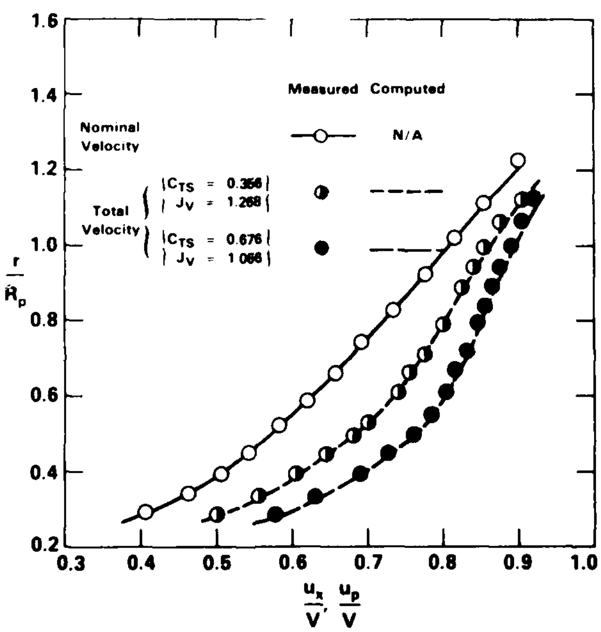

Figure 8 – Measured and Computed Axial Velocity Profiles Immediately Upstream of Propulsor (x/D_p = −0.239) With and Without Propulsor T Operated in Wake C

TABLE 1 – OFFSETS FOR MODEL 1

x/L*	y/L	y/R**	x/L	y/L	y/R	x/L	y/L	y/R
0.00000	0.00000	0.00000	.2[illegible]	[illegible]	.5[illegible]	.7[illegible]2	.04274	.46[illegible]08
.00447	.00449	.10467	.27[illegible]	.0[illegible]	.5[illegible]	.74769	.04207	.46174
.00944	.01421	.15592	.28[illegible]	.04556	.5[illegible]	.75527	.04150	.45636
.01491	.01747	.19175	.2[illegible]	.04556	.5[illegible]	.76604	.040[illegible]	.44753
.01988	.02023	.22207	.3[illegible]	.04556	.50000	.77801	.03[illegible]	.43777
.02485	.02267	.24474	.3[illegible]	.04556	.5[illegible]	.78551	.03425	.43074
.02982	.02465	.27272	.3[illegible]	.04556	.50000	.7[illegible]	.03421	.41937
.03479	.02684	[illegible]	.3[illegible]	.04556	.5[illegible]	.8[illegible]	.03[illegible]	.41123
.03976	.02866	.31453	.3[illegible]	[illegible]	.5[illegible]	.8[illegible]	.03[illegible]28	.39814
.04473	.03037	.33297	.3[illegible]	.04556	.50000	.82726	.03149	.38395
.04970	.03184	.35000	.3[illegible]	.04556	.50000	.82466	.03107	.37386
.05467	.03333	.36575	.3[illegible]	.04556	.5[illegible]	.84621	.03260	.35773
.05964	.03466	.38034	.3[illegible]	.04536	.50000	.85710	.03101	.34014
.06461	.03588	.39383	.3[illegible]	.04556	.5[illegible]	.86518	.02489	.32800
.06958	.03702	.40629	.4[illegible]	.04536	.5[illegible]	.87655	.02[illegible]10	.30035
.07455	.03807	[illegible]	.4[illegible]	[illegible]	.50000	.88413	.02[illegible]83	.29443
.07952	.03901	.42833	.4[illegible]	[illegible]	.5[illegible]	.89550	.02481	.27247
.08449	.03991	.43800	.4[illegible]	[illegible]	.5[illegible]	.9[illegible]	.02264	.24448
.08946	.04071	.44682	.4[illegible]	[illegible]	.5[illegible]	.91445	.02[illegible]	.23166
.09443	.04134	[illegible]	.4[illegible]	[illegible]	.5[illegible]	.92145	.01889	.20736
.09940	.04210	.46205	.4[illegible]	[illegible]	.5[illegible]	.92[illegible]	.01[illegible]	.18182
.10437	.04266	[illegible]	.4[illegible]	[illegible]	.5[illegible]	.94433	.01[illegible]	.15391
.10934	.04322	[illegible]	.4[illegible]	[illegible]	[illegible]	.95[illegible]	.01[illegible]	.13364
.11431	.04384	[illegible]	.4[illegible]	[illegible]	[illegible]	.95[illegible]26	.01[illegible]	.11900
.11928	.04403	.48178	.5[illegible]	.045[illegible]	.5[illegible]	.96[illegible]	.00[illegible]	.10470
.12425	.04433	.48757	.5[illegible]	[illegible]	.5[illegible]	.96421	.00[illegible]	.09500
.12922	.04472	[illegible]	.5[illegible]	[illegible]	.5[illegible]	.96620	.00[illegible]	.08491
.13419	.04495	[illegible]	.5[illegible]	[illegible]	[illegible]	.9[illegible]	.00[illegible]	.08145
.13917	.04516	[illegible]	.5[illegible]	[illegible]	[illegible]	.9[illegible]	.00[illegible]	.08[illegible]
.14414	.04531	.49[illegible]	[illegible]	[illegible]	[illegible]	.9[illegible]	.00[illegible]	.07[illegible]
.14911	.04542	[illegible]	.5[illegible]	[illegible]	[illegible]	.9[illegible]	.00[illegible]	.07[illegible]
.15408	.04550	[illegible]	.5[illegible]	[illegible]	[illegible]	.9[illegible]	[illegible]	[illegible]
.15905	.04553	[illegible]	.5[illegible]	[illegible]	[illegible]	.9[illegible]	.00[illegible]	.06[illegible]64
.1640[illegible]	.04556	[illegible]	.5[illegible]	[illegible]	.5[illegible]	.9[illegible]	.00[illegible]	[illegible]
.16899	.04556	.50000	.6[illegible]	.04556	[illegible]	.9[illegible]	.00[illegible]	.06164
.17396	.04556	.50000	.6[illegible]	[illegible]	[illegible]	.98[illegible]	.00	.06109
.17893	.04556	.50000	.62[illegible]2	.0451[illegible]	.49[illegible]	.98[illegible]	.00[illegible]	.05[illegible]
.18390	.04556	.50000	.6[illegible]	[illegible]	.49[illegible]	.98[illegible]	.00[illegible]4	.05[illegible]36
.1893[illegible]	.04556	.50000	.6[illegible]	[illegible]	.49[illegible]	.98[illegible]	.004[illegible]	.05[illegible]55
.19383	.04556	.50000	.6[illegible]	.04[illegible]	.49[illegible]	.98807	.00164	.05091
.19881	.04556	.50000	.6[illegible]	.04517	.49[illegible]	.99216	.00133	.04[illegible]55
.20875	.04556	.50000	.6[illegible]	.04501	.49416	.99225	.00301	.04420
.21869	.04556	.50000	.6[illegible]05	.04475	.49[illegible]	.99424	.00156	.03909
.22863	.04556	.50000	.6[illegible]	.04441	.48741	.99602	.00284	.03127
.23857	.04556	.50000	.7[illegible]	.04415	.48448	.99801	.00188	.02064
.24851	.04556	.50000	.7[illegible]	.04368	.47940	1.00000	0.00000	0.00000
.25845	.04556	.50000	.72435	.04333	.47555			

*L = Total Hull Length

**R = Maximum Hull Radius

TABLE 2 – OFFSETS FOR MODEL C

X/L*	Y/L	Y/R**	X/L	Y/L	Y/R	X/L	Y/L	Y/R
0.00000	0.00000	0.00000	.05143	.03204	.35804	.22171	.04475	.50000
.00002	.00057	.00642	.05503	.03306	.36939	.22531	.04475	.50000
.00006	.00115	.01284	.05864	.03402	.38015	.23892	.04475	.50000
.00014	.00172	.01924	.06224	.03494	.39035	.24252	.04475	.50000
.00026	.00229	.02563	.06585	.03580	.40002	.24613	.04475	.50000
.00040	.00286	.03201	.06945	.03662	.40917	.24973	.04475	.50000
.00057	.00343	.03835	.07308	.03739	.41781	.25406	.04475	.50000
.00078	.00400	.04467	.07667	.03812	.42596	.25925	.04475	.50000
.00101	.00456	.05095	.08027	.03881	.43362	.26548	.04475	.50000
.00128	.00512	.05719	.08388	.03945	.44081	.27296	.04475	.50000
.00157	.00567	.06338	.08748	.04005	.44753	.28193	.04475	.50000
.00189	.00622	.06953	.09109	.04061	.45380	.29270	.04475	.50000
.00223	.00677	.07562	.09469	.04113	.45961	.30562	.04475	.50000
.00261	.00731	.08165	.09830	.04161	.46497	.32112	.04475	.50000
.00300	.00784	.08762	.10190	.04205	.46990	.32972	.04475	.50000
.00342	.00837	.09351	.10551	.04246	.47440	.36205	.04475	.50000
.00386	.00889	.09934	.10912	.04282	.47848	.38061	.04475	.50000
.00432	.00940	.10508	.11272	.04315	.48214	.39958	.04475	.50000
.00481	.00991	.11075	.11633	.04344	.48541	.41834	.04475	.50000
.00529	.01041	.11632	.11993	.04370	.48829	.42710	.04475	.50000
.00580	.01090	.12181	.12354	.04393	.49080	.45587	.04475	.50000
.00632	.01138	.12719	.12714	.04412	.49295	.47463	.04475	.50000
.00686	.01186	.13248	.13075	.04428	.49476	.49339	.04475	.50000
.00741	.01232	.13767	.13435	.04441	.49625	.51216	.04475	.50000
.00797	.01277	.14274	.13796	.04452	.49744	.52092	.04475	.50000
.00853	.01322	.14770	.14157	.04460	.49836	.54968	.04475	.50000
.00910	.01365	.15255	.14517	.04466	.49904	.56844	.04475	.50000
.00967	.01408	.15727	.14878	.04470	.49950	.58721	.04475	.50000
.01025	.01449	.16187	.15238	.04473	.49979	.60597	.04475	.50000
.01082	.01489	.16635	.15599	.04474	.49994	.62474	.04475	.49983
.01139	.01528	.17070	.15959	.04475	.49999	.64350	.04437	.49875
.01197	.01566	.17495	.16320	.04475	.50000	.66226	.04341	.49660
.01254	.01603	.17909	.16680	.04475	.50000	.68102	.04178	.49355
.01312	.01639	.18314	.17041	.04475	.50000	.69979	.04248	.47467
.01369	.01675	.18710	.17402	.04475	.50000	.71855	.04152	.46396
.01427	.01709	.19098	.17762	.04475	.50000	.73731	.04040	.45142
.01484	.01743	.19478	.18123	.04475	.50000	.75608	.03911	.43698
.01553	.01783	.19924	.18483	.04475	.50000	.77484	.03764	.42057
.01636	.01830	.20446	.18844	.04475	.50000	.79360	.03598	.40207
.01735	.01884	.21056	.19204	.04475	.50000	.81237	.03413	.38132
.01853	.01948	.21764	.19565	.04475	.50000	.83113	.03206	.35815
.01997	.02021	.22583	.19926	.04475	.50000	.84989	.02975	.33236
.02169	.02106	.23523	.20286	.04475	.50000	.86866	.02718	.30371
.02374	.02203	.24611	.20647	.04475	.50000	.88742	.02434	.27195
.02621	.02313	.25847	.21007	.04475	.50000	.90618	.02114	.23682
.02918	.02439	.27251	.21368	.04475	.50000	.92495	.01772	.19802
.03274	.02581	.28835	.21728	.04475	.50000	.94371	.01340	.15526
.03700	.02740	.30611	.22089	.04475	.50000	.96247	.00969	.10822
.04061	.02866	.32018	.22349	.04475	.50000	.98124	.00506	.05656
.04422	.02985	.33348	.22410	.04475	.50000	1.00000	0.00000	0.00000
.0478	.0310	.3461						

*L = Total Hull Length

**R = Maximum Hull Radius

TABLE 3 – OFFSETS FOR MODEL D

X/L*	Y/L	Y/R**	X/L	Y/L	Y/R	X/L	Y/L	Y/R
0.00000	0.00000	0.00000	.22323	.04736	.50000	.65566	.04736	.50000
.00529	.01071	.11309	.22681	.04736	.50000	.66601	.04736	.50000
.01058	.01515	.15992	.24340	.04736	.50000	.67637	.04736	.50000
.01587	.01855	.19582	.24698	.04736	.50000	.68672	.04736	.50000
.02116	.02140	.22600	.24956	.04736	.50000	.69708	.04736	.50000
.02540	.02343	.24742	.25214	.04736	.50000	.70743	.04736	.50000
.02963	.02529	.26702	.25571	.04736	.50000	.71778	.04736	.50000
.03386	.02701	.28515	.25929	.04736	.50000	.72814	.04736	.50000
.03704	.02852	.29993	.31749	.04736	.50000	.73849	.04736	.50000
.04445	.03082	.32540	.31847	.04736	.50000	.74885	.04736	.50000
.05241	.03337	.35339	.32106	.04736	.50000	.76057	.04736	.50000
.05820	.03498	.36929	.33164	.04736	.50000	.76854	.04736	.50000
.06349	.03638	.38307	.34422	.04736	.50000	.78036	.04736	.50000
.06879	.03767	.39779	.35480	.04736	.50000	.79218	.04736	.50000
.07408	.03888	.41051	.37039	.04736	.50000	.80006	.04736	.50000
.07937	.03999	.42225	.38097	.04736	.50000	.81188	.04736	.50000
.08466	.04102	.43306	.39155	.04736	.50000	.82369	.04736	.50000
.08995	.04195	.44296	.40213	.04736	.50000	.83157	.04736	.50000
.09524	.04280	.45195	.41272	.04736	.50000	.84339	.04736	.50000
.10053	.04357	.46008	.42330	.04736	.50000	.85127	.04736	.50000
.10582	.04426	.46735	.43388	.04736	.50000	.86309	.04736	.50000
.11112	.04487	.47379	.43446	.04736	.50000	.87490	.04736	.50000
.11641	.04541	.47941	.43505	.04736	.50000	.88278	.04736	.50000
.12170	.04586	.48424	.43563	.04736	.50000	.89460	.04736	.50000
.12699	.04625	.48834	.43621	.04736	.50000	.90642	.04736	.50000
.13228	.04657	.49171	.43680	.04736	.50000	.91430	.04736	.50000
.13757	.04683	.49437	.43738	.04736	.50000	.92611	.04736	.50000
.14286	.04702	.49634	.43796	.04736	.50000	.93399	.04736	.50000
.14815	.04717	.49763	.43855	.04736	.50000	.94581	.04736	.50000
.15345	.04726	.49831	.43913	.04736	.50000	.95763	.04736	.50000
.15874	.04732	.49862	.43971	.04736	.50000	.96551	.04736	.50000
.16403	.04735	.49881	.44030	.04736	.50000	.97541	.04736	.50000
.16932	.04735	.50000	.44088	.04736	.50000	.98347	.04736	.50000
.17461	.04736	.50000	.44146	.04736	.50000	.98858	.04736	.50000
.17990	.04736	.50000	.44205	.04736	.50000	.99147	.04736	.50000
.18519	.04736	.50000	.44263	.04736	.50000	.99341	.04736	.50000
.19048	.04736	.50000	.44320	.04736	.50000	.99533	.04736	.50000
.19578	.04736	.50000	.44378	.04736	.50000	.99688	.04736	.50000
.20107	.04736	.50000	.44437	.04736	.50000	.99853	.04736	.50000
.20636	.04736	.50000	.44495	.04736	.50000	.99920	.04736	.50000
.21165	.04736	.50000	.44510	.04736	.50000	1.00000	0.00000	0.00000

*L = Total Hull Length

**R = Maximum Hull Radius

TABLE 4 – COMPUTED GROSS EFFECTIVE WAKE PARAMETERS AND MEASURED TAYLOR'S WAKE FRACTION AT VARIOUS PROPULSION CONDITIONS IN THE FIVE WAKES

WAKE	J_V	C_{TS}	K_T	(1 t)	K_Q		$\eta_D \frac{(1-t)J_V K_T}{2\pi K_Q}$		$2\,C_{fo}$	MEASURED $(1-w_T)$	CALCULATED $(u_J)_{J_V}$	CALCULATED $(u_J)_{0.7}V$	PROPULSOR
					MEASURED	CALCULATED	MEASURED	CALCULATED					
1	1.25	0.370	0.227	0.920		0.0453		0.919	0.013	0.685	0.676	0.672	1
$(u_J)_{J_V}/V=0.840$	1.07	0.654	0.295	0.920		0.0558		0.830	0.013	0.695	0.689	0.683	
A	0.416	3.616	0.246	1.00		0.0326		0.500	0.0145	0.798	0.831	0.834	J
$(u_J)_{J_V}/V=0.702$	0.666	0.965	0.168	1.00		0.0263		0.677	0.0164	0.777	0.804	0.806	
B	0.456	3.02	0.247	1.00		0.0328		0.547	0.0148	0.772	0.752	0.752	J
$(u_J)_{J_V}/V=0.688$	0.745	0.765	0.167	1.00		0.0266		0.749	0.0167	0.697	0.725	0.687	
C	1.268	0.356	0.225	0.911	0.0475	0.0460	0.870	0.898	0.0125	0.694	0.694	0.694	1
$(u_J)_{J_V}/V=0.695$	1.157	0.498	0.262	0.911	0.0520	0.0513	0.857	0.856	0.0123	0.704	0.699	0.698	
	1.066	0.676	0.302	0.911	0.0574	0.0578	0.813	0.808	0.0122	0.706	0.704	0.704	
D	1.290	0.360	0.236	0.893	0.0490	0.0465	0.871	0.918	0.0125	0.667	0.642	0.642	1
$(u_J)_{J_V}/V=0.815$	1.174	0.500	0.270	0.891	0.0532	0.0514	0.847	0.874	0.0124	0.681	0.655	0.649	
	1.054	0.706	0.308	0.901	0.0574	0.0565	0.811	0.823	0.0121	0.695	0.661	0.654	

TABLE 5 – TOTAL AND EFFECTIVE AXIAL VELOCITY PROFILES COMPUTED FROM NOMINAL AND PROPULSOR INDUCED AXIAL VELOCITIES AT THE LOCATION OF PROPULSOR

(a) PROPULSOR T IN WAKE 1. C_{TS} = 0.370, J_V = 1.25

INPUT				OUTPUT			
NOMINAL		INDUCED		TOTAL		EFFECTIVE	
r/R_p	u_x/V	u_a/V	u_{tp}/V	r_p/R_p	u_p/V	r/R_p	u_a/V
0.211	0.313	0.088	0.082	0.211	0.564	0.211	0.476
0.250	0.354	0.152	0.093	0.233	0.660	0.250	0.490
0.300	0.396	0.214	0.083	0.263	0.736	0.300	0.521
0.350	0.434	0.254	0.067	0.296	0.786	0.350	0.542
0.400	0.470	0.280	0.053	0.328	0.840	0.400	0.561
0.450	0.502	0.315	0.031	0.362	0.894	0.450	0.579
0.500	0.530	0.323	0.008	0.390	0.918	0.500	0.595
0.550	0.560	0.320	0.013	0.436	0.933	0.550	0.613
0.600	0.590	0.303	0.036	0.474	0.934	0.600	0.631
0.650	0.620	0.268	-0.063	0.515	0.919	0.650	0.651
0.700	0.650	0.205	-0.084	0.560	0.877	0.700	0.672
0.750	0.680	0.149	0.108	0.600	0.844	0.750	0.695
0.800	0.710	0.099	0.121	0.650	0.819	0.800	0.720
0.850	0.738	0.073	0.111	0.712	0.818	0.850	0.745
0.900	0.762	0.054	-0.101	0.766	0.821	0.900	0.767
0.950	0.786	0.039	0.093	0.821	0.829	0.950	0.790
1.000	0.810	0.030	0.084	0.878	0.843	1.000	0.813
1.050	0.834	0.023	0.074	0.931	0.859	1.050	0.836
1.100	0.856	0.017	0.066	0.985	0.874	1.100	0.900
1.200	0.900	0.010	0.052	1.094	0.910	1.200	0.925
1.300	0.925	0.006	0.042	1.202	0.931	1.500	0.960
1.500	0.960	0.003	0.300	1.415	0.963		
2.000	1.000						

(b) PROPULSOR T IN WAKE 1 C_{TS} 0.654 J_V 1.07

0.211	0.313	0.090	0.119	0.211	0.597	0.211	0.507
0.250	0.354	0.161	0.129	0.232	0.690	0.250	0.529
0.300	0.396	0.245	0.126	0.280	0.795	0.300	0.550
0.350	0.434	0.322	0.107	0.289	0.891	0.350	0.569
0.400	0.470	0.368	0.091	0.320	0.954	0.400	0.586
0.450	0.502	0.400	0.056	0.351	1.010	0.450	0.602
0.500	0.530	0.427	0.029	0.383	1.043	0.500	0.616
0.550	0.560	0.427	0.001	0.417	1.059	0.550	0.632
0.600	0.590	0.425	0.040	0.453	1.073	0.600	0.649
0.650	0.620	0.396	-0.002	0.491	1.061	0.650	0.665
0.700	0.650	0.321	-0.129	0.531	1.004	0.700	0.683
0.750	0.680	0.232	-0.184	0.576	0.936	0.750	0.704
0.800	0.710	0.162	-0.188	0.625	0.889	0.800	0.727
0.850	0.738	0.126	-0.174	0.677	0.870	0.850	0.750
0.900	0.762	0.095	-0.166	0.731	0.865	0.900	0.770
0.950	0.786	0.072	-0.155	0.786	0.864	0.950	0.792
1.000	0.810	0.055	-0.140	0.841	0.869	1.000	0.814
1.050	0.834	0.037	-0.123	896	0.874	1.050	0.837
1.100	0.856	0.027	-0.109	0.952	0.885	1.100	0.858
1.200	0.900	0.015	-0.086	1.064	0.910	1.200	0.901
1.300	0.925	0.008	-0.070	1.174	0.934	1.300	0.926
1.500	0.960	0.005	-0.040	1.391	0.965	1.500	0.960
2.000	1.000		-0.024				

TABLE 6 – COMPUTED RESULTS OF PROPULSOR/WAKE INTERACTION

(a) PROPULSOR T IN WAKE 1

WAKE 1									
		C_{TS} = 0.370, J_V = 1.25				C_{TS} = 0.864, J_V = 1.07			
$\frac{r}{R_p}$	$\frac{u_a}{V}$	$\frac{u_a}{V}$	$\frac{u_a}{V}$	$\tan\beta_i$	G	$\frac{u_a}{V}$	$\frac{u_a}{V}$	$\tan\beta_i$	G
0.211	0.313	0.000	0.476	0.910	0.0000	0.000	0.587	0.847	0.0000
0.25	0.364	0.152	0.486	0.794	0.0029	0.101	0.529	0.706	0.0038
0.30	0.388	0.214	0.521	0.707	0.0060	0.246	0.560	0.733	0.0078
0.40	0.476	0.286	0.561	0.748	0.0110	0.300	0.595	0.719	0.0150
0.50	0.538	0.323	0.595	0.670	0.0100	0.427	0.616	0.657	0.0222
0.60	0.599	0.383	0.631	0.501	0.0179	0.425	0.640	0.504	0.0257
0.70	0.658	0.266	0.672	0.510	0.0172	0.321	0.683	0.511	0.0250
0.80	0.710	0.000	0.720	0.462	0.0140	0.162	0.727	0.443	0.0224
0.90	0.762	0.864	0.767	0.300	0.0006	0.006	0.770	0.377	0.0153
0.95	0.786	0.830	0.790	0.361	0.0053	0.872	0.792	0.345	0.0103
1.00	0.810	0.830	0.813	0.334	0.0000	0.856	0.814	0.316	0.0000
1.05	0.834	0.823	0.836		0.0000	0.837	0.837	-	0.0000
1.10	0.856	0.817	0.857		0.0000	0.827	0.858	-	0.0000
1.20	0.900	0.810	0.900		0.0000	0.815	0.900	-	0.0000

(b) PROPULSOR J IN WAKE A

WAKE A									
		C_{TS} 0.986, J_V 0.886				C_{TS} 3.82, J_V 0.416			
$\frac{r}{R_p}$	$\frac{u_a}{V}$	$\frac{u_a}{V}$	$\frac{u_a}{V}$	$\tan\beta_i$	G	$\frac{u_a}{V}$	$\frac{u_a}{V}$	$\tan\beta_i$	G
0.182	0.528	0.000	0.000	1.114	0.0000	0.291	0.730	1.135	0.0000
0.250	0.585	0.383	0.000	0.000	0.0153	0.751	0.755	0.004	0.0346
0.300	0.603	0.434	0.705	0.772	0.0286	0.002	0.705	0.753	0.0404
0.400	0.644	0.404	0.732	0.501	0.0200	1.026	0.783	0.567	0.0004
0.500	0.000	0.400	0.757	0.401	0.0204	1.051	0.000	0.400	0.0047
0.600	0.735	0.466	0.783	0.400	0.0291	1.030	0.017	0.303	0.0071
0.700	0.777	0.422	0.000	0.340	0.0200	0.002	0.034	0.325	0.0000
0.800	0.016	0.362	0.034	0.305	0.0254	0.003	0.052	0.277	0.0007
0.900	0.040	0.256	0.057	0.200	0.0100	0.000	0.000	0.237	0.0400
0.950	0.053	0.103	0.000	0.253	0.0147	0.525	0.001	0.224	0.0374
1.000	0.076	0.105	0.000	0.230	0.0000	0.270	0.005	0.200	0.0000
1.050	0.000	0.000	0.000	-	0.0000	0.000	0.000	-	0.0000
1.100	0.000	0.000	0.000	-	0.0000	0.000	0.000	-	0.0000
1.200	0.024	0.000	0.000	-	0.0000	0.000	0.000	-	0.0000

TABLE 6 – COMPUTED RESULTS OF PROPULSOR/WAKE INTERACTION

(c) PROPULSOR J IN WAKE B

WAKE B									
$\frac{r}{R_p}$	$\frac{u_x}{V}$	$C_{TS} = 0.765$, $J_V = 0.745$				$C_{TS} = 3.02$, $J_V = 0.458$			
		$\frac{u_\theta}{V}$	$\frac{u_\theta}{V}$	$\tan\beta_i$	G	$\frac{u_\theta}{V}$	$\frac{u_\theta}{V}$	$\tan\beta_i$	G
0.182	0.544	0.000	0.639	1.148	0.0000	0.050	0.693	1.144	0.0000
0.250	0.566	0.335	0.646	0.924	0.0133	0.668	0.699	0.891	0.0311
0.300	0.587	0.386	0.652	0.786	0.0181	0.813	0.703	0.750	0.0417
0.400	0.598	0.436	0.669	0.602	0.0233	0.933	0.715	0.567	0.0530
0.500	0.630	0.434	0.687	0.487	0.0257	0.957	0.727	0.455	0.0586
0.600	0.663	0.422	0.706	0.413	0.0265	0.944	0.739	0.384	0.0614
0.700	0.694	0.377	0.725	0.350	0.0253	0.905	0.752	0.325	0.0607
0.800	0.727	0.319	0.746	0.305	0.0227	0.814	0.766	0.277	0.0561
0.900	0.760	0.227	0.770	0.267	0.0173	0.586	0.783	0.239	0.0452
0.950	0.776	0.163	0.783	0.252	0.0128	0.427	0.792	0.223	0.0343
1.000	0.792	0.090	0.797	0.239	0.0000	0.252	0.803	0.117	0.0000
1.050	0.806	0.000	0.000		0.0000	0.000	0.000	-	0.0000
1.100	0.820	0.000	0.000		0.0000	0.000	0.000	-	0.0000
1.200	0.842	0.000	0.000		0.0000	0.000	0.000	-	0.0000

(d) PROPULSOR IN WAKE C

WAKE C													
$\frac{r}{R_p}$	$\frac{u_x}{V}$	$C_{TS} = 0.358$, $J_V = 1.268$				$C_{TS} = 0.498$, $J_V = 1.157$				$C_{TS} = 0.676$, $J_V = 1.066$			
		$\frac{u_\theta}{V}$	$\frac{u_\theta}{V}$	$\tan\beta_i$	G	$\frac{u_\theta}{V}$	$\frac{u_\theta}{V}$	$\tan\beta_i$	G	$\frac{u_\theta}{V}$	$\frac{u_\theta}{V}$	$\tan\beta_i$	G
0.211	0.387	0.000	0.512	0.945	0.0000	0.078	0.526	0.947	0.0000	0.106	0.542	0.913	0.0000
0.250	0.417	0.142	0.531	0.844	0.0023	0.147	0.545	0.787	0.0028	0.170	0.559	0.755	0.0035
0.300	0.464	0.202	0.564	0.834	0.0051	0.225	0.586	0.780	0.0059	0.251	0.589	0.747	0.0071
0.400	0.528	0.279	0.583	0.776	0.0107	0.321	0.604	0.747	0.0127	0.367	0.615	0.732	0.0152
0.500	0.579	0.315	0.629	0.686	0.0150	0.378	0.637	0.680	0.0182	0.445	0.646	0.674	0.0220
0.600	0.631	0.292	0.662	0.614	0.0172	0.346	0.668	0.603	0.0213	0.410	0.675	0.601	0.0261
0.700	0.677	0.204	0.694	0.535	0.0168	0.244	0.698	0.526	0.0214	0.302	0.704	0.524	0.0266
0.800	0.720	0.095	0.729	0.483	0.0140	0.123	0.732	0.453	0.0184	0.161	0.736	0.451	0.0235
0.900	0.763	0.056	0.766	0.388	0.0088	0.077	0.770	0.387	0.0123	0.102	0.772	0.381	0.0164
0.950	0.785	0.042	0.788	0.388	0.0055	0.057	0.790	0.356	0.0081	0.076	0.791	0.350	0.0112
1.000	0.806	0.031	0.809	0.340	0.0000	0.043	0.809	0.327	0.0000	0.056	0.810	0.319	0.0000
1.050	0.826	0.000	0.000	-	0.0000	0.000	0.000	-	0.0000	0.000	0.000	-	0.0000
1.100	0.845	0.000	0.000		0.0000	0.000	0.000	-	0.0000	0.000	0.000	-	0.0000
1.200	0.880	0.000	0.000		0.0000	0.000	0.000	-	0.0000	0.000	0.000	-	0.0000

TABLE 6 – COMPUTED RESULTS OF PROPULSOR/WAKE INTERACTION

(e) PROPULSOR T IN WAKE D

WAKE D													
$\frac{r}{R_p}$	$\frac{u_x}{V}$	$C_{TS} = 0.388$, $J_V = 1.290$				$C_{TS} = 0.588$, $J_V = 1.174$				$C_{TS} = 0.788$, $J_V = 1.064$			
		$\frac{u_a}{V}$	$\frac{u_t}{V}$	$\tan\beta_i$	G	$\frac{u_a}{V}$	$\frac{u_t}{V}$	$\tan\beta_i$	G	$\frac{u_a}{V}$	$\frac{u_t}{V}$	$\tan\beta_i$	G
0.211	0.360	0.071	0.484	0.957	0.0000	0.078	0.501	0.904	0.0000	0.074	0.515	0.843	0.0000
0.250	0.388	0.122	0.501	0.794	0.0022	0.143	0.517	0.748	0.0027	0.155	0.532	0.698	0.0035
0.300	0.420	0.196	0.521	0.790	0.0050	0.217	0.536	0.741	0.0058	0.244	0.549	0.688	0.0070
0.400	0.468	0.279	0.548	0.743	0.0109	0.320	0.562	0.717	0.0128	0.374	0.574	0.691	0.0154
0.500	0.516	0.330	0.575	0.670	0.0155	0.387	0.587	0.656	0.0185	0.462	0.597	0.642	0.0226
0.600	0.567	0.293	0.606	0.593	0.0178	0.355	0.615	0.584	0.0217	0.431	0.623	0.576	0.0269
0.700	0.620	0.205	0.642	0.520	0.0175	0.257	0.649	0.512	0.0219	0.323	0.654	0.505	0.0276
0.800	0.672	0.097	0.683	0.452	0.0145	0.129	0.688	0.443	0.0188	0.173	0.691	0.435	0.0243
0.900	0.722	0.060	0.728	0.389	0.0092	0.082	0.731	0.378	0.0126	0.112	0.732	0.367	0.0170
0.950	0.745	0.046	0.749	0.360	0.0057	0.062	0.752	0.348	0.0083	0.088	0.752	0.336	0.0115
1.000	0.767	0.034	0.770	0.331	0.0000	0.047	0.771	0.318	0.0000	0.064	0.772	0.305	0.0000
1.050	0.790	0.000	0.000	–	0.0000	0.000	0.000	–	0.0000	0.000	0.000	–	0.0000
1.100	0.811	0.000	0.000	–	0.0000	0.000	0.000	–	0.0000	0.000	0.000	–	0.0000
1.200	0.849	0.000	0.000	–	0.0000	0.000	0.000	–	0.0000	0.000	0.000	–	0.0000

TABLE 7 – MEASURED AND COMPUTED VELOCITY PROFILES IMMEDIATELY UPSTREAM OF PROPULSOR WITH AND WITHOUT AN OPERATING PROPULSOR

(a) AT X/D_p = -0.227, PROPULSOR T IN WAKE 1, C_{TS} = 0.370, J_V = 1.25

MEASURED NOMINAL VELOCITY*			INPUT				PROPELLER TOTAL VELOCITY			
					COMPUTED		COMPUTED		MEASURED	
$\frac{r}{R_p}$	$\frac{u_x}{V}$	$\frac{v_r}{V}$	$\frac{r}{R_p}$	$\frac{u_x}{V}$	$\frac{u_a}{V}$	$\frac{v_M}{V}$	$\frac{r_p}{R_p}$	$\frac{u_p}{V}$	$\frac{r_p}{R_p}$	$\frac{u_p}{V}$
0.262	0.318	-0.033	0.250	0.324	0.0388	0.0091	0.2500	0.4411	0.280	0.480
0.274	0.334	-0.039	0.300	0.377	0.0435	0.0130	0.2887	0.4859	0.350	0.554
0.284	0.345	-0.041	0.350	0.420	0.0519	0.0150	0.3300	0.5281	0.424	0.613
0.294	0.360	-0.042	0.400	0.458	0.0619	0.0122	0.3727	0.5685	0.499	0.659
0.314	0.381	-0.046	0.450	0.490	0.0698	0.0050	0.4163	0.6023	0.574	0.698
0.334	0.400	-0.047	0.500	0.522	0.0757	-0.0017	0.4606	0.6344	0.634	0.722
0.364	0.428	-0.055	0.550	0.551	0.0793	-0.0108	0.5056	0.6620	0.699	0.745
0.405	0.459	-0.055	0.600	0.583	0.0808	-0.0201	0.5512	0.6903	0.769	0.788
0.435	0.483	-0.049	0.650	0.614	0.0787	-0.0288	0.5976	0.7146	0.836	0.805
0.487	0.524	-0.049	0.700	0.644	0.0740	-0.0356	0.6447	0.7360	0.900	0.825
0.528	0.545	-0.045	0.750	0.675	0.0683	-0.0412	0.6926	0.7576	0.983	0.849
0.588	0.585	-0.045	0.800	0.704	0.0619	-0.0456	0.7412	0.7773	1.065	0.880
0.649	0.620	-0.044	0.850	0.732	0.0552	-0.0478	0.7903	0.7962	1.166	0.912
0.720	0.661	-0.040	0.900	0.758	0.0486	-0.0487	0.8400	0.8136	1.322	0.950
0.782	0.701	-0.036	0.950	0.783	0.0420	-0.0485	0.8901	0.8305	1.510	0.973
0.868	0.742	-0.033	1.000	0.807	0.0362	-0.0472	0.9406	0.8474		
0.954	0.790	-0.035	1.050	0.830	0.0308	-0.0455	0.9914	0.8640		
1.036	0.827	-0.033	1.100	0.852	0.0263	-0.0433	1.0423	0.8807		
1.157	0.880	-0.038	1.200	0.896	0.0192	-0.0385	1.1446	0.9164		
1.270	0.915	-0.028	1.300	0.925	0.0141	-0.0339	1.2472	0.9398		
1.391	0.947	-0.029	1.500	0.960	0.0083	-0.0258	1.4521	0.9685		
1.514	0.960	-0.025	2.000	1.000	0.0026	-0.0154				
1.625	0.970	-0.020								

(b) AT X D_p -0.227 PROPULSOR T IN WAKE 1, C_{TS} = 0.654, J_V = 1.07

0.262	0.318	-0.033	0.250	0.324	0.0652	0.0195	0.2500	0.5025	0.280	0.554
0.274	0.334	-0.039	0.300	0.377	0.0748	0.0230	0.2844	0.5475	0.334	0.611
0.284	0.345	-0.041	0.350	0.420	0.0889	0.0231	0.3219	0.5917	0.391	0.656
0.294	0.360	-0.042	0.400	0.458	0.1027	0.0178	0.3613	0.6327	0.460	0.706
0.314	0.381	-0.046	0.450	0.490	0.1143	0.0079	0.4019	0.6677	0.529	0.751
0.334	0.400	-0.047	0.500	0.522	0.1228	-0.0049	0.4435	0.6999	0.612	0.787
0.364	0.428	-0.055	0.550	0.551	0.1282	-0.0187	0.4860	0.7271	0.695	0.818
0.405	0.459	-0.055	0.600	0.583	0.1290	-0.0326	0.5294	0.7524	0.772	0.837
0.435	0.483	-0.049	0.650	0.614	0.1268	-0.0465	0.5738	0.7737	0.851	0.853
0.487	0.524	-0.049	0.700	0.644	0.1191	-0.0574	0.6193	0.7909	0.923	0.870
0.528	0.545	-0.045	0.750	0.675	0.1107	-0.0664	0.6659	0.8081	1.025	0.898
0.588	0.585	-0.045	0.800	0.704	0.1010	-0.0734	0.7134	0.8229	1.145	0.924
0.649	0.620	-0.044	0.850	0.732	0.0903	-0.0772	0.7618	0.8364	1.310	0.955
0.720	0.661	-0.040	0.900	0.758	0.0795	-0.0788	0.8110	0.8486	1.481	0.973
0.782	0.701	-0.036	0.950	0.783	0.0689	-0.0789	0.8609	0.8606		
0.868	0.742	-0.033	1.000	0.807	0.0588	-0.0773	0.9113	0.8725		
0.954	0.790	-0.035	1.050	0.830	0.0505	-0.0746	0.9623	0.8856		
1.036	0.827	-0.033	1.100	0.852	0.0430	-0.0711	1.0136	0.8988		
1.157	0.880	-0.038	1.200	0.896	0.0311	-0.0631	1.1168	0.9290		
1.270	0.915	-0.028	1.300	0.925	0.0227	-0.0552	1.2206	0.9487		
1.391	0.947	-0.029	1.500	0.960	0.0131	-0.0421	1.4279	0.9735		
1.514	0.960	-0.025	2.000	1.000	0.0046	-0.0253				
1.625	0.970	-0.020								

*( ) MEASURED ALONG HORIZONTAL PLANE
OTHERWISE MEASURED ALONG VERTICAL PLANE

TABLE 7 – MEASURED AND COMPUTED VELOCITY PROFILES IMMEDIATELY UPSTREAM OF PROPULSOR WITH AND WITHOUT AN OPERATING PROPULSOR (Continued)

(c) AT $X/D_p = -0.336$, PROPULSOR J IN WAKE A, $C_{TS} = 0.965$, $J_V = 0.666$

MEASURED NOMINAL VELOCITY		INPUT				PROPELLER TOTAL VELOCITY				
				COMPUTED		COMPUTED		MEASURED		
$\frac{r}{R_p}$	$\frac{u_x}{V}$	$\frac{r}{R_p}$	$\frac{u_x}{V}$	$\frac{u_a}{V}$	$\frac{v_{pr}}{V}$	$\frac{r_p}{R_p}$	$\frac{u_p}{V}$	$\frac{r_p}{R_p}$	$\frac{u_p}{V}$	$\frac{v_{pr}}{V}$
0.0000	0.514	0.00	0.515	0.0941	0.0000	0.0000	0.6653			
0.1537	0.513	0.05	0.501	0.0941	-0.0018	0.0438	0.6546			
0.3074	0.573	0.10	0.503	0.0941	-0.0041	0.0876	0.6561			
0.4610	0.672	0.15	0.514	0.0941	-0.0065	0.1315	0.6646			
0.6147	0.745	0.20	0.526	0.0941	-0.0090	0.1758	0.6739	0.6147	(0.821)	(-0.029)
0.7684	0.810	0.25	0.548	0.0941	-0.0106	0.2205	0.6912			
0.9221	0.850	0.30	0.570	0.0941	-0.0145	0.2656	0.7088	0.9221	(0.900)	(-0.059)
1.0758	0.895	0.35	0.597	0.0940	-0.0176	0.3113	0.7306			
1.2294	0.931	0.40	0.631	0.0938	-0.0207	0.3576	0.7584	1.2294	0.973 (0.956)	-0.044 (-0.056)
1.3831	0.956	0.45	0.666	0.0930	-0.0242	0.4044	0.7870	1.3831	0.988	-0.039
1.5368	0.982	0.50	0.692	0.0918	-0.0275	0.4516	0.8079	1.5368	0.999 (0.986)	-0.032 (-0.043)
1.6905	0.986	0.55	0.720	0.0902	-0.0315	0.4992	0.8304	1.6905	0.997	-0.026
1.8442	0.984	0.60	0.741	0.0880	-0.0349	0.5471	0.8465	1.8442	0.987	-0.017
1.9978	0.989	0.65	0.762	0.0854	-0.0380	0.5952	0.8624	1.9978	0.994	-0.017
2.1515	0.982	0.70	0.782	0.0825	-0.0409	0.6436	0.8773	2.1515	0.992	-0.013
2.3052	0.985	0.75	0.802	0.0791	-0.0440	0.6922	0.8918	2.3052	0.995	-0.011
		0.80	0.820	0.0756	-0.0462	0.7410	0.9045			
		0.85	0.834	0.0708	-0.0481	0.7901	0.9125			
		0.90	0.846	0.0664	-0.0496	0.8393	0.9191			
		0.95	0.860	0.0618	-0.0508	0.8888	0.9274			
		1.00	0.874	0.0569	-0.0510	0.9385	0.9355			
		1.10	0.898	0.0464	-0.0509	1.0881	0.9496			
		1.20	0.924	0.0400	-0.0490	1.1383	0.9659			
		1.30	0.943	0.0332	-0.0465	1.2393	0.9774			
		1.50	0.969	0.0224	-0.0395	1.4421	0.9918			
		1.70	0.982	0.0154	-0.0331	1.6454	0.9976			
		2.00	0.990	0.0129	-0.0262	1.9500	1.0030			

(d) AT $X/D_p = -0.336$, PROPULSOR J IN WAKE A, $C_{TS} = 3.62$, $J_V = 0.417$

0.0000	0.514	0.00	0.515	0.272	0.000	0.0000	0.9088			
0.1537	0.513	0.05	0.501	0.272	-0.004	0.0374	0.9010			
0.3074	0.573	0.10	0.503	0.272	-0.012	0.0747	0.9021			
0.4610	0.672	0.15	0.514	0.272	-0.019	0.1123	0.9083			
0.6147	0.745	0.20	0.526	0.271	-0.028	0.1503	0.9141	0.6147	(1.011)	(-0.096)
0.7684	0.810	0.25	0.548	0.270	-0.036	0.1890	0.9260			
0.9221	0.850	0.30	0.570	0.269	-0.045	0.2285	0.9382	0.9221	(1.025)	(-0.136)
1.0758	0.895	0.35	0.597	0.268	-0.054	0.2689	0.9538			
1.2294	0.931	0.40	0.631	0.267	-0.062	0.3101	0.9745	1.2294	1.051 (1.024)	-0.116 (-0.138)
1.3831	0.956	0.45	0.666	0.263	-0.072	0.3524	0.9935	1.3831	1.043	0.104
1.5368	0.982	0.50	0.692	0.259	-0.082	0.3955	1.0072	1.5368	1.032 (1.026)	-0.098 (-0.102)
1.6905	0.986	0.55	0.720	0.254	-0.092	0.4393	1.0217	1.6905	1.026	-0.077
1.8442	0.984	0.60	0.741	0.247	-0.101	0.4837	1.0296	1.8442	1.013	-0.062
1.9978	0.989	0.65	0.762	0.239	-0.111	0.5286	1.0369	1.9978	1.009	-0.054
2.1515	0.982	0.70	0.782	0.229	-0.118	0.5741	1.0417	2.1515	1.001	-0.045
2.3052	0.985	0.75	0.802	0.218	-0.126	0.6201	1.0459	2.3052	1.007	-0.041
		0.80	0.820	0.206	-0.132	0.6668	1.0479			
		0.85	0.834	0.194	-0.137	0.7140	1.0468			
		0.90	0.846	0.182	-0.141	0.7616	1.0446			
		0.95	0.860	0.170	-0.143	0.8097	1.0440			
		1.00	0.874	0.156	-0.144	0.8583	1.0416			
		1.10	0.898	0.132	-0.143	0.9569	1.0381			
		1.20	0.924	0.108	-0.137	1.0572	1.0369			
		1.30	0.943	0.0890	-0.139	1.1589	1.0350			
		1.50	0.969	0.0608	-0.111	1.3644	1.0301			
		1.70	0.982	0.0415	-0.090	1.5715	1.0240			
		2.00	0.990	0.0325	-0.078	1.8813	1.0227			

TABLE 7 – MEASURED AND COMPUTED VELOCITY PROFILES IMMEDIATELY UPSTREAM OF PROPULSOR WITH AND WITHOUT AN OPERATING PROPULSOR (Continued)

(e) AT X/D_p = -0.489, PROPULSOR J IN WAKE A, C_{TS} = 3.62, J_V = 0.416

MEASURED NOMINAL VELOCITY		INPUT				PROPELLER TOTAL VELOCITY				
				COMPUTED		COMPUTED		MEASURED		
$\frac{r}{R_p}$	$\frac{u_x}{V}$	$\frac{r}{R_p}$	$\frac{u_x}{V}$	$\frac{u_a}{V}$	$\frac{v_{tr}}{V}$	$\frac{r_p}{R_p}$	$\frac{u_p}{V}$	$\frac{r_p}{R_p}$	$\frac{u_p}{V}$	$\frac{v_{tr}}{V}$
0.0000	0.511	0.00	0.511	0.1930	0.0000	0.0000	0.8010			
0.1537	0.509	0.05	0.502	0.1927	-0.0058	0.0398	0.7950			
0.3074	0.577	0.10	0.500	0.1920	-0.0117	0.0795	0.7930	0.3074	0.825	-0.004
0.4610	0.665	0.15	0.508	0.1912	-0.0173	0.1194	0.7973	0.4610	0.895	-0.030
0.6147	0.750	0.20	0.526	0.1899	-0.0228	0.1598	0.8076	0.6147	0.952	-0.056
0.7684	0.789	0.25	0.548	0.1894	-0.0271	0.2009	0.8216	0.7684	0.989	-0.072
0.9221	0.851	0.30	0.571	0.1863	-0.0330	0.2428	0.8340	0.9221	1.014	-0.077
1.0758	0.891	0.35	0.596	0.1844	-0.0390	0.2855	0.8495	1.0758	1.037	-0.080
1.2294	0.930	0.40	0.621	0.1820	-0.0439	0.3288	0.8648	1.2294	1.051	-0.077
1.5368	0.978	0.45	0.646	0.1798	-0.0493	0.3728	0.8808	1.5368	1.036	-0.061
1.8442	0.984	0.50	0.670	0.1750	-0.0546	0.4174	0.8938	1.8442	1.027	-0.048
2.1515	0.987	0.55	0.690	0.1710	-0.0590	0.4625	0.9049	2.1515	1.017	-0.037
		0.60	0.713	0.1655	-0.0640	0.5081	0.9171			
		0.65	0.734	0.1608	-0.0685	0.5542	0.9289			
		0.70	0.755	0.1557	-0.0715	0.6008	0.9405			
		0.75	0.778	0.1500	-0.0758	0.6478	0.9534			
		0.80	0.801	0.1440	-0.0785	0.6953	0.9663			
		0.85	0.820	0.1372	-0.0819	0.7432	0.9754			
		0.90	0.840	0.1308	-0.0841	0.7914	0.9859			
		0.95	0.857	0.1240	-0.0858	0.8400	0.9937			
		1.00	0.872	0.1171	-0.0870	0.8889	0.9998			
		1.10	0.901	0.1040	-0.0879	0.9876	1.0122			
		1.20	0.925	0.0922	-0.0868	1.0871	1.0220			
		1.30	0.943	0.0803	-0.0853	1.1873	1.0265			
		1.50	0.975	0.0605	-0.0783	1.3894	1.0365			
		1.70	0.985	0.0455	-0.0697	1.5929	1.0309			
		2.00	0.993	0.0342	-0.0580	1.8985	1.0273			

(f) AT X/D_p = -0.336, PROPULSOR J IN WAKE B, C_{TS} = 0.765, J_V = 0.745

0.0000	0.506	0.00	0.506	0.0830	0.0000	0.0000	0.6316			
0.1537	0.527	0.05	0.508	0.0833	-0.0021	0.0448	0.6335			
0.3074	0.571	0.10	0.516	0.0837	-0.0039	0.0896	0.6403			
0.4610	0.615	0.15	0.530	0.0840	-0.0062	0.1347	0.6519			
0.6147	0.656 (0.637)	0.20	0.541	0.0841	-0.0081	0.1801	0.6610	0.6147	(0.730)	(-0.021)
0.7684	0.692	0.25	0.556	0.0842	-0.0109	0.2257	0.6734			
0.9221	0.737 (0.704)	0.30	0.568	0.0842	-0.0135	0.2715	0.6834	0.9221	(0.790)	(-0.054)
1.0758	0.790	0.35	0.584	0.0841	-0.0161	0.3176	0.6966			
1.2294	0.838 (0.818)	0.40	0.597	0.0839	-0.0185	0.3639	0.7074	1.2294	0.882 (0.861)	-0.034 (-0.052)
1.3831	0.872	0.45	0.610	0.0829	-0.0216	0.4104	0.7174	1.3831	0.924	-0.037
1.5368	0.910 (0.893)	0.50	0.624	0.0819	-0.0245	0.4571	0.7283	1.5368	0.947 (0.943)	-0.027 (-0.051)
1.6905	0.947	0.55	0.637	0.0808	-0.0275	0.5041	0.7384	1.6905	0.969	-0.022
1.8442	0.969	0.60	0.650	0.0783	-0.0308	0.5513	0.7472	1.8442	0.982	-0.015
1.9978	0.972	0.65	0.664	0.0762	-0.0339	0.5988	0.7573	1.9978	0.983	-0.011
2.1515	0.968	0.70	0.676	0.0738	-0.0369	0.6465	0.7654	2.1515	0.986	-0.009
2.3052	0.980	0.75	0.689	0.0706	-0.0392	0.6944	0.7738	2.3052	0.986	-0.005
		0.80	0.704	0.0669	-0.0412	0.7427	0.7835			
		0.85	0.717	0.0631	-0.0431	0.7912	0.7914			
		0.90	0.732	0.0588	-0.0445	0.8400	0.8000			
		0.95	0.747	0.0545	-0.0454	0.8892	0.8103			
		1.00	0.762	0.0505	-0.0460	0.9385	0.8201			
		1.10	0.795	0.0426	-0.0455	1.0380	0.8431			
		1.20	0.826	0.0348	-0.0439	1.1383	0.8648			
		1.30	0.854	0.0288	-0.0413	1.2392	0.8856			
		1.50	0.907	0.0198	-0.0358	1.4421	0.9281			
		1.70	0.951	0.0132	-0.0291	1.6455	0.9647			
		2.00	0.983	0.0102	-0.0217	1.9505	0.9933			

TABLE 7 – MEASURED AND COMPUTED VELOCITY PROFILES IMMEDIATELY UPSTREAM OF PROPULSOR WITH AND WITHOUT AN OPERATING PROPULSOR (Continued)

(g) AT X/D_p = -0.336, PROPULSOR J IN WAKE B, C_{TS} = 3.02, J_V = 0.456

MEASURED NOMINAL VELOCITY		INPUT				PROPELLER TOTAL VELOCITY				
				COMPUTED		COMPUTED		MEASURED		
$\frac{r}{R_p}$	$\frac{u_x}{V}$	$\frac{r}{R_p}$	$\frac{u_x}{V}$	$\frac{u_a}{V}$	$\frac{v_{pr}}{V}$	$\frac{r_p}{R_p}$	$\frac{u_p}{V}$	$\frac{r_p}{R_p}$	$\frac{u_p}{V}$	$\frac{v_{pr}}{V}$
0.0000	0.506	0.00	0.506	0.243	0.000	0.0000	0.8458			
0.1537	0.527	0.05	0.508	0.244	-0.005	0.0387	0.8480			
0.3074	0.571	0.10	0.516	0.245	-0.012	0.0775	0.8538			
0.4610	0.615	0.15	0.530	0.246	-0.018	0.1167	0.8634			
0.6147	0.650 (0.637)	0.20	0.541	0.246	-0.025	0.1564	0.8701	0.6147	(0.884)	(-0.083)
0.7684	0.692	0.25	0.556	0.246	-0.032	0.1964	0.8796			
0.9221	0.730 (0.784)	0.30	0.568	0.245	-0.040	0.2388	0.8862	0.9221	(0.896)	(-0.122)
1.0758	0.790	0.35	0.584	0.244	-0.048	0.2776	0.8955			
1.2294	0.830 (0.810)	0.40	0.597	0.242	-0.056	0.3189	0.9021	1.2294	0.958 (0.934)	-0.105 (-0.127)
1.3831	0.872	0.45	0.610	0.239	-0.064	0.3607	0.9077	1.3831	0.983	-0.093
1.5368	0.918 (0.893)	0.50	0.624	0.237	-0.074	0.4028	0.9152	1.5368	1.000 (0.978)	-0.084 (-0.102)
1.6905	0.947	0.55	0.637	0.232	-0.083	0.4453	0.9192	1.6905	1.008	-0.069
1.8442	0.969	0.60	0.650	0.225	-0.093	0.4884	0.9213	1.8442	0.994	-0.052
1.9978	0.972	0.65	0.664	0.216	-0.101	0.5321	0.9222	1.9978	0.981	-0.047
2.1515	0.968	0.70	0.676	0.209	-0.108	0.5763	0.9239	2.1515	0.988	-0.044
2.3052	0.980	0.75	0.689	0.200	-0.115	0.6210	0.9245	2.3052	0.991	-0.038
		0.80	0.704	0.188	-0.121	0.6664	0.9238			
		0.85	0.717	0.178	-0.125	0.7124	0.9238			
		0.90	0.732	0.167	-0.129	0.7590	0.9246			
		0.95	0.747	0.154	-0.132	0.8063	0.9236			
		1.00	0.762	0.142	-0.133	0.8543	0.9239			
		1.10	0.795	0.119	-0.131	0.9520	0.9286			
		1.20	0.826	0.099	-0.125	1.0518	0.9356			
		1.30	0.854	0.082	-0.118	1.1532	0.9436			
		1.50	0.907	0.054	-0.100	1.3590	0.9645			
		1.70	0.951	0.038	-0.083	1.5670	0.9903			
		2.00	0.983	0.028	-0.064	1.8783	1.0112			

(h) AT X/D_p = -0.239, PROPULSOR T IN WAKE C, C_{TS} = 0.356, J_V = 1.268

0.291	0.411	0.260	0.375	0.0368	0.0070	0.260	0.472	0.285	0.500	
0.341	0.462	0.300	0.423	0.0405	0.0109	0.293	0.514	0.332	0.555	
0.392	0.506	0.350	0.473	0.0473	0.0120	0.336	0.563	0.391	0.604	
0.447	0.542	0.400	0.510	0.0560	0.0104	0.380	0.600	0.446	0.646	
0.520	0.582	0.450	0.543	0.0628	0.0050	0.425	0.637	0.495	0.681	
0.587	0.620	0.500	0.572	0.0691	-0.0023	0.470	0.669	0.530	0.701	
0.660	0.658	0.550	0.600	0.0720	-0.0107	0.516	0.695	0.610	0.742	
0.741	0.692	0.600	0.628	0.0724	-0.0182	0.562	0.720	0.667	0.756	
0.826	0.735	0.650	0.652	0.0708	-0.0248	0.609	0.740	0.716	0.776	
0.920	0.777	0.700	0.675	0.0675	-0.0315	0.656	0.757	0.795	0.803	
1.018	0.815	0.750	0.698	0.0628	-0.0363	0.704	0.773	0.836	0.812	
1.105	0.853	0.800	0.722	0.0578	-0.0399	0.753	0.789	0.889	0.828	
1.226	0.899	0.850	0.745	0.0518	-0.0423	0.801	0.805	0.942	0.841	
		0.900	0.767	0.0457	-0.0438	0.851	0.819	0.997	0.855	
		0.950	0.788	0.0403	-0.0440	0.901	0.833	1.065	0.877	
		1.000	0.809	0.0352	-0.0432	0.951	0.848	1.125	0.905	
		1.050	0.831	0.0303	-0.0419	1.001	0.864			
		1.100	0.852	0.0261	-0.0401	1.051	0.880			
		1.200	0.908	0.0193	-0.0361	1.153	0.920			

TABLE 7 – MEASURED AND COMPUTED VELOCITY PROFILES IMMEDIATELY UPSTREAM OF PROPULSOR WITH AND WITHOUT AN OPERATING PROPULSOR (Continued)

(i) AT X/D_p = -0.239, PROPULSOR T IN WAKE C, C_{TS} = 0.676, J_V = 1.066

MEASURED NOMINAL VELOCITY		INPUT				PROPELLER TOTAL VELOCITY			
				COMPUTED		COMPUTED		MEASURED	
$\frac{r}{R_p}$	$\frac{u_x}{V}$	$\frac{r}{R_p}$	$\frac{u_x}{V}$	$\frac{u_a}{V}$	$\frac{v_w}{V}$	$\frac{r_p}{R_p}$	$\frac{u_p}{V}$	$\frac{r_p}{R_p}$	$\frac{u_p}{V}$
0.291	0.411	0.260	0.375	0.0728	0.0163	0.260	0.542	0.285	0.576
0.341	0.462	0.300	0.423	0.0812	0.0179	0.289	0.585	0.332	0.631
0.392	0.506	0.350	0.473	0.0920	0.0176	0.328	0.632	0.391	0.689
0.447	0.542	0.400	0.510	0.1047	0.0108	0.368	0.673	0.446	0.726
0.520	0.582	0.450	0.543	0.1148	0.0017	0.410	0.708	0.495	0.761
0.587	0.620	0.500	0.572	0.1217	-0.0103	0.452	0.737	0.530	0.777
0.660	0.658	0.550	0.600	0.1243	-0.0230	0.496	0.762	0.610	0.803
0.741	0.692	0.600	0.628	0.1240	-0.0351	0.540	0.784	0.667	0.816
0.826	0.735	0.650	0.652	0.1218	-0.0464	0.585	0.801	0.716	0.831
0.920	0.777	0.700	0.675	0.1147	-0.0562	0.630	0.813	0.795	0.846
1.018	0.815	0.750	0.698	0.1076	-0.0640	0.677	0.825	0.836	0.854
1.105	0.853	0.800	0.722	0.0985	-0.0698	0.724	0.836	0.889	0.866
1.226	0.899	0.850	0.745	0.0890	-0.0737	0.772	0.847	0.942	0.874
		0.900	0.767	0.0781	-0.0758	0.821	0.856	0.997	0.890
		0.950	0.788	0.0689	-0.0759	0.870	0.865	1.065	0.905
		1.000	0.809	0.0600	-0.0754	0.920	0.876	1.125	0.920
		1.050	0.831	0.0522	-0.0727	0.971	0.888		
		1.100	0.852	0.0448	-0.0698	1.022	0.901		
		1.200	0.900	0.0330	-0.0627	1.124	0.935		

(j) AT X D_p -0.239, PROPULSOR T IN WAKE D, C_{TS} = 0.706, J_V = 1.054

0.255	0.387	0.220	0.366	0.0711	0.0179	0.220	0.530	0.304	0.596
0.370	0.452	0.250	0.386	0.0757	0.0205	0.241	0.549	0.391	0.657
0.444	0.487	0.300	0.414	0.0878	0.0210	0.279	0.581	0.462	0.699
0.525	0.530	0.350	0.441	0.0100	0.0197	0.321	0.524	0.565	0.744
0.607	0.572	0.400	0.467	0.1129	0.0123	0.363	0.647	0.636	0.766
0.680	0.606	0.450	0.492	0.1232	0.0019	0.404	0.675	0.715	0.795
0.763	0.657	0.500	0.516	0.1310	-0.0108	0.445	0.701	0.794	0.811
0.852	0.694	0.550	0.542	0.1346	-0.0241	0.486	0.723	0.871	0.826
0.978	0.756	0.600	0.567	0.1341	-0.0370	0.529	0.742	0.930	0.846
1.071	0.795	0.650	0.592	0.1306	-0.0501	0.573	0.758	0.975	0.855
1.170	0.842	0.700	0.618	0.1238	-0.0608	0.618	0.772	1.020	0.865
1.283	0.875	0.750	0.644	0.1156	-0.0690	0.664	0.784	1.071	0.875
		0.800	0.670	0.1061	-0.0753	0.711	0.797	1.145	0.892
		0.850	0.696	0.0957	-0.0792	0.759	0.808	1.244	0.905
		0.900	0.721	0.0842	-0.0820	0.807	0.819		
		0.950	0.745	0.0856	-0.0821	0.856	0.831		
		1.000	0.768	0.0643	-0.0808	0.906	0.841		
		1.050	0.790	0.0558	-0.0784	0.957	0.852		
		1.100	0.810	0.0479	-0.0752	1.008	0.863		
		1.200	0.850	0.0351	-0.0675	1.111	0.888		

ACKNOWLEDGMENTS

The investigation reported herein was funded under the David W. Taylor Naval Ship R&D Center's Independent Research Program, Task Area ZR 0230101, Element No. 61152N. The authors would like to thank their co-workers, Messrs. N. Santelli and G. Belt for velocity measurements, Messrs. R.P. Cross, L.B. Crook, and W.G. Day Jr. for self-propulsion experiments, Mr. D.H. Fuhs and Dr. B. Cox for practical applications of the present theory, and Mr. J.H. McCarthy and Dr. William B. Morgan for their continuous support and technical guidance. The authors wish to express their gratitude to Dr. T. Nagamatsu and Dr. K. Tokunaga of Nagasaki Experimental Tank, Japan, for providing detailed information of their experiments and data.

REFERENCES

1. Huang, T.T., H.T. Wang, N. Santelli, and N.C. Groves, "Propeller/Stern Boundary Layer Interaction on Axisymmetric Bodies: Theory and Experiment," David W. Taylor Naval Ship Research and Development Center Report 76-0113 (Dec 1976).

2. Nagamatsu, T. and K. Tokunaga, "Prediction of *Effective Wake Distribution for a Body of Revolution*," Journal of Society of Naval Architects of Japan, Vol. 143, pp. 93-100.

3. Schetz, J.A. and S. Favin, "Numerical Solution for the Near Wake of a Body with Propeller," Journal of Hydronautics, Vol. 11, No. 4, pp. 136-141 (Oct 1977).

4. Schetz, J.A. and S. Favin, "Numerical Solution of a Body-Propeller Combination Flow Including Swirl and Comparisons with Data," Journal of Hydronautics, Vol. 13, No. 2, pp. 46-51 (April 1979).

5. Hucho, W.H., "Über den Einfluss einer Heckschraube auf die Druckverteilung und die Grenzschicht eines Rotationskörpers - Teil II: Untersuchungen bei hoheren Schubbelastungsgraden," Institut Für Stromungsmechanik der Technischen Hochschule Branunschweig, Bericht 64/45 (1965).

6. Hucho, W.H., "Über den Zusammenhang zwischen Normalsog, Reibungssog und dem Nachstrom bei der Strömung um Rotationskörper," Schiff und Hafen, Heft 10, pp. 689-693 (1968).

7. Hucho, W.H., "Untersuchungen über den Einfluss einer Heckschraube auf die Druckverteilung und die Grenzschicht Schiffsähnlicher Körper," Ingenieur-Archiv Vol. XXXVII, pp. 288-303 (1969).

8. Wertbrecht, H.M., "Vom Sog, ein Versuch Seiner Berechnung," Jahrbuch Schiffbautechnische Gesellschaft, Vol. 42, pp. 147-204 (1941).

9. Hickling, R., "Propellers in the Wake of an Axisymmetric Body," Transactions of the Royal Institute of Naval Architects, Vol. 99, pp. 601-617 (1957).

10. Tsakonas, S. and Jacobs, W.R., "Potential and Viscous Parts of the Thrust Deduction and Wake Fraction for an Ellipsoid of Revolution," Journal of Ship Research, Vol. 4, No. 2, pp. 1-16 (1960).

11. Wald, Q., "Performance of a Propeller in a Wake and the Interaction of Propeller and Hull," Journal of Ship Research, Vol. 9, No. 1, pp. 1-8 (1965).

12. Raestad, A.E., "Estimation of Marine Propeller's Induced Effects on the Hull Wake-Scale Effect on the Hull Wake Field," Det norske Veritas Report No. 72-3-M, Chapter 1 (1972).

13. Nagamatsu, T. and T. Sasajima, "Effect of Propeller Suction on Wake," Journal of the Society of Naval Architects of Japan, Vol. 137, pp. 58-63 (1975).

14. Titoff, I.A. and Otlesnov, Yu. P., "Some Aspects of Propeller-Hull Interaction," Swedish-Soviet Propeller Symposium, Moscow (1975).

15. Thwaites, B., *Incompressible Aerodynamics*, Chapter XI, Oxford University Press (1960).

16. Huang, T.T., N. Santelli, and G. Belt, "Stern Boundary-Layer Flow on Axisymmetric Bodies," Twelfth Symposium on Naval Hydrodynamics 5-9 June 1978, Printed by National Academy of Sciences, Wash., D.C., pp. 127-157 (1979).

17. Hough, G.R. and D.E. Ordway, "The Generalized Actuator Disk," Developments in Theoretical and Applied Mechanics, Vol. 11, Pergamon Press, New York, pp. 317-336, Table 1 (1965).

18. Morgan, W.B. and J.W. Wrench, "Some Computational Aspects of Propeller Design," Methods in Computational Physics, Vol. 4, Academic Press, New York, pp. 301-331 (1965).

19. Caster, E.B., J.A. Diskin, and T.A. LaFone, "A Lifting Line Computer Program For Preliminary Design of Propellers," DTNSRDC Ship Performance Department Report No. SPD-595-01 (Nov 1975).

20. Kerwin, J.E. and L. Leopold, "A Design Theory for Subcavitating Theory," Transactions of the Society of Naval Architects and Marine Engineers, Vol. 72, pp. 294-335 (1964).

21. Huang, T.T. and B.D. Cox, "Interaction of After body Boundary Layer and Propeller," paper presented at Symposium on Hydrodynamics of Ship and Offshore Propulsion Systems, Sponsored by Det Norske Veritas, Hovix outside Oslo, (March 20-25, 1977).

22. Cheng, H.M., "Hydrodynamic Aspects of Propeller Design Based on Lifting Surface Theory, Parts 1 and 2," DTMB Report 1802 and 1803 (1964-1965).

23. Kerwin, J.E., "Computer Techniques for Propeller Blade Section," International Shipbuilding Progresses, Vol. 20, No. 227, pp. 227-251 (July 1973).

24. Cummings, D.E., "Numerical Prediction of Propeller Characteristics," Journal of Ship Research, Vol. 17, Part 3, pp. 12-18 (1973).

INITIAL DISTRIBUTION

Copies	
1	WES
1	U.S. ARMY TRAS R&D Marine Trans Div
1	CHONR/438 Cooper
2	NRL 1 Code 2027 1 Code 2629
1	ONR/Boston
1	ONR/Chicago
1	ONR/New York
1	ONR/Pasadena
1	ONR/San Francisco
1	NORDA
3	USNA 1 Tech Lib 1 Nav Sys Eng Dept 1 B. Johnson
3	NAVPGSCOL 1 Lib 1 T. Sarpkaya 1 J. Miller
1	NADC
1	NOSC/Lib
1	NSWC, White Oak/Lib
1	NSWC, Dahlgren/Lib
1	NUSC/Lib

Copies	
15	NAVSEA 1 SEA 033 1 SEA 03D 1 SEA 05T 1 SEA 05H 1 SEA 312 1 SEA 32 1 SEA 321 1 SEA 32R 1 SEA 521 1 SEA 524 1 SEA 62P 1 SEA 6661 (Blount) 3 SEA 996
12	DTIC
1	AFOSR/NAM
1	AFFOL/FYS, J. Olsen
2	MARAD 1 Div of Ship R&D 1 Lib
1	NASA/HQ/Lib
1	NASA/Ames Res Ctr, Lib
2	NASA/Langley Res Ctr 1 Lib 1 D. Bushnell
3	NBS 1 Lib 1 P.S. Klebanoff 1 G. Kulin
1	NSF/Eng Lib
1	DOT/Lib TAD-491.1
2	MMA 1 National Maritime Research Center 1 Lib

Copies	
4	U of Cal/Dept Naval Arch, Berkeley 1 Lib 1 W. Webster 1 J. Paulling 1 J. Wehausen
3	CIT 1 Aero Lib 1 T.Y. Wu 1 A.J. Acosta
1	Colorado State U/Eng Res Cen
1	Cornell U/Shen
2	Harvard U 1 G. Carrier 1 Gordon McKay Lib
4	U of Iowa 1 Lib 1 L. Landweber 1 J. Kennedy 1 V.C. Patel
4	MIT 1 Lib 1 J.R. Kerwin 1 P. Leehey 1 J.N. Newman
2	U of Minn/St. Anthony Falls 1 Lib 1 R. Arndt
3	U of Mich/NAME 1 Lib 1 F. Ogilivie 1 Cough
3	Penn State 1 B.R. Parkin 1 R.E. Henderson 1 ARL Lib
1	Princeton U/Mellor

Copies	
1	U of Rhode Island 1 F.M. White
1	Science Application, Inc. Annapolis, MD C. von Kerczek
2	SIT 1 Lib 1 Breslin
3	Stanford U 1 Eng Lib 1 R. Street, Dept Civil Eng 1 S.J. Kline, Dept Mech Eng
1	U of VA/Aero Eng Dept
1	VPI 1 J. Schetz, Dept Aero & Ocean Eng
3	Webb Inst 1 Library 1 Lewis 1 Ward
1	SNAME/Tech Lib
1	Bell Aerospace
2	Boeing Company/Seattle 1 Marine System 1 P. Rubbert
1	Bolt, Beranek & Newman/Lib
1	Exxon, NY/Design Div Tank Dept
1	Exxon Math & System, Inc.
1	General Dynamics, EB/ Boatwright
1	Flow Research
1	Gibbs & Cox/Tech Info

Copies	
1	Grumman Aerospace Corp/Lib
5	Hydronautics 1 Lib 1 E. Miller 1 V. Johnson 1 C.C. Hsu 1 M. Tulin
1	Lockheed, Sunnyvale/Waid
2	McDonnell Douglas, Long Beach 1 T. Cebeci 1 J. Hess
1	Northrop Corp/Aircraft Div
1	Sun Shipbuilding/Chief Naval Arch
1	United Technology/East Hartford, Conn.
1	Westinghouse Electric 1 M.S. Macovsky

Copies	Code	Name
5	1552	N.C. Groves
1	1552	H.T. Wang
1	1552	M.S. Chang
1	1561	C.M. Lee
1	1564	J. Feldman
1	1568	G. Cox
1	1606	T.C. Tai
1	1840	J. Schot
1	1843	H. Haussling
1	19	M.M. Sevik
1	1940	J.T. Shen
1	1942	F. Archibald
1	1942	B.E. Bowers
1	1946	J.A. Padgett
10	5211.1	Reports Distribution
1	522.1	Unclassified Lib (C)
1	522.2	Unclassified Lib (A)

CENTER DISTRIBUTION

Copies	Code	Name
1	1500	W.B. Morgan
1	152	W.C. Lin
1	1524	W. Day
1	1532	M. Wilson
1	154	J. McCarthy
1	1542	B. Yim
1	1543	R. Cumming
1	1544	T. Brockett
1	1544	R. Boswell
1	1544	. Lin
30	1552	T.T. Huang

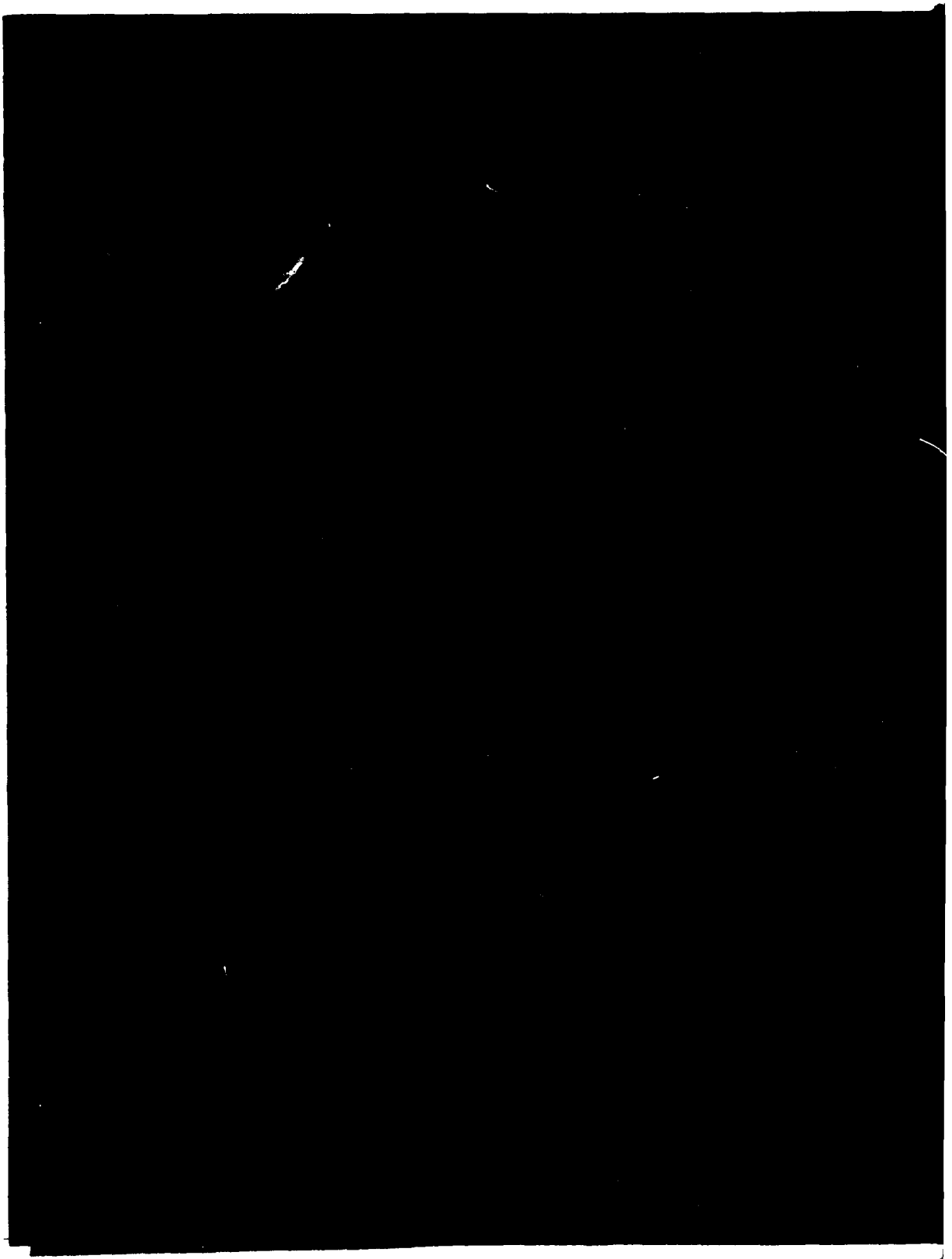

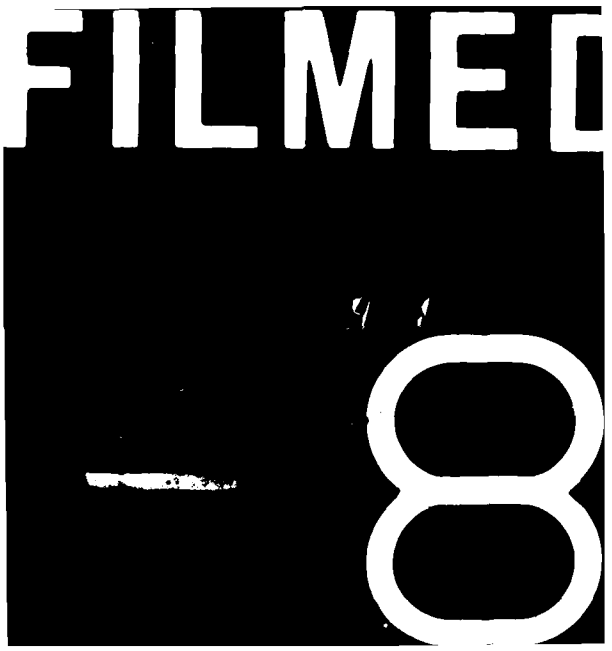
FILME
8